Engineering 20 (2023) 77–95

Contents lists available at ScienceDirect

Engineering

journal homepage: www.elsevier.com/locate/eng

Research
Intelligent Medicine—Review

# Progress of Brain Network Studies on Anesthesia and Consciousness: Framework and Clinical Applications

Jun Liu [a,*], Kangli Dong [a], Yi Sun [b], Ioannis Kakkos [c], Fan Huang [a], Guozheng Wang [a], Peng Qi [d,*], Xing Chen [a], Delin Zhang [e], Anastasios Bezerianos [f], Yu Sun [a,b,*]

[a] Key Laboratory for Biomedical Engineering of Ministry of Education of China, Zhejiang University, Hangzhou 310007, China
[b] Department of Neurology, Sir Run Run Shaw Hospital, School of Medicine, Zhejiang University, Hangzhou 310020, China
[c] School of Electrical and Computer Engineering, National Technical University of Athens, Athens 15780, Greece
[d] Department of Control Science and Engineering, College of Electronics and Information Engineering, Tongji University, Shanghai 200092, China
[e] Department of Anesthesiology, The First Affiliated Hospital, School of Medicine, Zhejiang University, Hangzhou 310003, China
[f] The N1 Institute for Health, Center for Life Sciences, National University of Singapore, Singapore 117456, Singapore

ARTICLE INFO

*Article history:*
Received 20 July 2021
Revised 21 October 2021
Accepted 9 November 2021
Available online 13 December 2021

*Keywords:*
Anesthesia
Brain network
Connectivity
Graph theoretical analysis
Clinical monitoring system

ABSTRACT

Although the relationship between anesthesia and consciousness has been investigated for decades, our understanding of the underlying neural mechanisms of anesthesia and consciousness remains rudimentary, which limits the development of systems for anesthesia monitoring and consciousness evaluation. Moreover, the current practices for anesthesia monitoring are mainly based on methods that do not provide adequate information and may present obstacles to the precise application of anesthesia. Most recently, there has been a growing trend to utilize brain network analysis to reveal the mechanisms of anesthesia, with the aim of providing novel insights to promote practical application. This review summarizes recent research on brain network studies of anesthesia, and compares the underlying neural mechanisms of consciousness and anesthesia along with the neural signs and measures of the distinct aspects of neural activity. Using the theory of cortical fragmentation as a starting point, we introduce important methods and research involving connectivity and network analysis. We demonstrate that whole-brain multimodal network data can provide important supplementary clinical information. More importantly, this review posits that brain network methods, if simplified, will likely play an important role in improving the current clinical anesthesia monitoring systems.



## 1. Introduction

### 1.1. General background

General anesthesia has been defined as the presence of unconsciousness, amnesia, and immobility [1]. This concept includes the suspension of not only the conscious activities performed by the brain, but also of the neurological and psychological factors mediated by the spinal cord. Every year, tens of millions of patients are placed under general anesthesia, which suppresses the treasured psychological attribute of consciousness. The ability of anesthesiologists to induce safe and reversible loss of consciousness (LOC) has proven invaluable. However, clinical monitoring systems for anesthesia are still lacking in their development, and the neurological mechanism of anesthetic-induced LOC remains unclear.

Research on unconsciousness under anesthesia has been conducted at both the micro- and macro-levels. At the micro-level, many studies have explored the mechanisms of action of general anesthetics on ion channels, receptors, and other molecules. Different anesthetics act on different molecular targets, which may play an important role in explaining various mechanisms of LOC caused by general anesthesia. The γ-aminobutyric acid type A (GABAA) receptor is the main inhibitory receptor in the brain and plays a pivotal role in LOC caused by general anesthetics. Researchers have found that mutations in the GABAA receptors alter the sensitivity of the brain towards anesthetics [2]. N-methyl-*D*-aspartic acid (NMDA) receptors, which are present in presynaptic and postsynaptic structures, are also targets of general anesthetics. Most inhaled anesthetics inhibit the NMDA receptors, but the level of inhibition differs for various anesthetics [3]. General anesthetics

* Corresponding authors.
*E-mail addresses:* liujun@zju.edu.cn (J. Liu), pqi@tongji.edu.cn (P. Qi), yusun@zju.edu.cn (Y. Sun).

https://doi.org/10.1016/j.eng.2021.11.013

can cause the opening of tandem two-pore potassium (K2Ps) channels. Studies have shown that K2P knockout mice have reduced sensitivity to inhaled anesthetics, suggesting that K2P channels are also the target of general anesthetics [4]. In addition to the three targets mentioned above, the effects of anesthetics on the brain are also mediated by other targets, which have not been fully studied [5].

At the macro-level, the development of neuroimaging technologies has enabled the investigation of the effects of anesthesia on multiple scales. However, the results from early anesthesia research and clinical testing are not as accurate as those reported more recently. Initially, anesthesia was studied primarily in the context of its clinical application and mainly depended on the measurement of the blood pressure, heart rate, respiration, and other physiological indicators. However, these indicators generally reflect indirect reactions caused by reduced levels of consciousness. In 1965, the minimum alveolar concentration (MAC) value was proposed as an indicator of the level of consciousness [6]. The MAC value is a measure that reflects the efficacy of inhalation anesthesia, which refers to the alveolar concentration of anesthetic gas necessary to prevent a bodily reaction to skin incisions in 50% of patients who inhaled anesthetic gas combined with pure oxygen at 1 atm (1 atm = 101 325 Pa) of pressure. However, the MAC value assesses anesthesia only at the somatic level and is merely an index of spinal nerve reflexes under noxious stimulation, which is not equivalent to unconsciousness [1,7,8] and is also affected by analgesic administration [9]. To overcome these limitations, researchers have recently attempted to investigate how anesthetics act on physiological targets [10] and to identify the mechanisms through which anesthetic drugs induce LOC.

Indirect reactions aside, the change in the brain's ability to integrate information is the direct physical correlation of a transition between consciousness states; such changes in integration should be the focus of our research. Based on recent neuroimaging studies, several different theories have been proposed to explain the mechanisms of anesthesia, including aberrations of cortical and thalamic connections [11–13], disrupted sleep–wake cycles [5,14,15], and cortical fragmentation [16,17]. Anesthetics can produce unconsciousness by blocking the interactions between specific brain regions and/or by reducing the transmission of information [18–20], and it has also been suggested that the cortex may represent the main target of anesthetics, given that the effect of both propofol and sevoflurane appears later in the subcortex compared with the cortex [21]. Notably, anesthetized and sleeping brains have long been revealed to show significant similarities; for example, the spindle waves observed during dexmedetomidine-induced sedation are similar to those that occur during normal sleep [22]. Natural sleep and wakefulness are controlled by multiple arousal pathways [23]. Anesthetics can affect the thalamus and cortex, suppress the wakefulness phase, and enhance the sleep phase. The sleep–wake cycle in the brain is a bistable system without an intermediate process, which coincides with the typically rapid return of wakefulness once anesthesia is discontinued [5]. Although general anesthetics can affect various targets in the sleep–wake cycle, the direct targets of these anesthetics remain to be elucidated [14]. Moreover, the neural mechanisms of general anesthetics, from molecular targets to the whole-brain level, remain unclear. General anesthetics can regulate the interactions between different brain regions by activating and/or inhibiting specific receptors within the central nervous system, eventually affecting the whole-brain networks and triggering reversible LOC.

In the study of anesthesia, various neuroimaging methods have been combined with network analyses. However, the clinical monitoring of anesthesia still lacks in its development and relies primarily on bodily reactions. Importantly, a lack of bodily reactions does not necessarily indicate unconsciousness. For anesthesia monitoring, unconsciousness should be judged from the perspective of connectivity (interaction between brain regions) [24]. The ideal monitoring equipment for assessing the depth of anesthesia (DOA) must meet the following requirements:

(1) Accurate monitoring of the patient's state of sedation and good correlation with clinical sedative performance;

(2) Accurate and reliable data;

(3) Compact equipment that is convenient to set-up and use;

(4) The ability to provide useful information to clinicians for decision-making;

(5) A lack of susceptibility to electromagnetic interference and interference from other equipment.

Unfortunately, the existing clinical anesthesia monitoring system does not meet these requirements. In practice, anesthesiologists often judge the DOA through observing the reactions of patients that is highly relying upon the empirical experience. There are various scoring criteria for the evaluation of the state of sedation, including the Ramsay Sedation Scale (RSS) [25], the Motor Activity Assessment Scale (MAAS) [26], and the Sedation–Agitation Scale (SAS) [27]. Scores on these scales are based on the patient's unresponsiveness to external disturbances, such as sound stimulation and noxious stimulation. Currently, the existing clinical anesthesia monitoring methods are far from meeting the prerequisites for precisely controlled anesthesia, and the risk of intraoperative wakefulness is relatively high. Unlike studies focused specifically on consciousness, the clinical application of anesthesia monitoring also needs to eliminate responses to noxious stimuli and prevent the patient from remembering any intraoperative events. Existing clinical anesthesia monitoring methods are not sufficiently accurate for the monitoring of consciousness, analgesia, and postoperative trauma. Additionally, individual differences have become a major obstacle to the precise application of anesthesia. Existing clinical anesthesia monitoring simplifies the complexity of brain monitoring for convenience, but also ignores much of the abundant information available for measurement within the brains of sedated patients. Hence, to meet the needs of anesthesia in the future, it is necessary to develop a method that takes advantage of this wealth of information, but it is also convenient to use in a clinical setting. Connectivity and network analysis based on electroencephalography (EEG) have provided us with a new idea for a system that directly reflects the change in consciousness at the whole-brain level, which offers great potential for developing comprehensive and holistic anesthesia monitoring and eliminating individual differences.

### 1.2. Aim and overview

This study reviews the development of brain connectivity research in the field of anesthesia, with a particular focus on the context of clinical anesthesia monitoring. Most of these studies investigated the mechanisms of anesthesia, from which we can obtain a clearer and more reliable understanding of anesthesia. A few studies have explored the combination of anesthesia mechanism research and clinical anesthesia monitoring. We performed an in-depth investigation and concluded that the study of brain functional connectivity (FC) and network during anesthesia is likely to give rise to clinical applications. To summarize the progress of anesthesia mechanism research in recent years and to identify the potential nexus of clinical monitoring and brain network research, this review focuses on the trends in the development of complex EEG-based network analyses in anesthesia and consciousness research over the last five years. In summary, this paper intends to highlight how brain FC and network analysis can be used to identify states of consciousness under anesthesia and propose future research directions that deserve attention to promote the development of anesthesia monitoring.

The main structure of this review is divided into the following four parts:

(1) We summarize the mechanism of anesthesia from both micro- and macro-scale perspectives. At the micro-level, we introduce the mechanism of general anesthetics at the level of molecular channels, receptors, and other molecules. At the macro-level, we discuss cortical and thalamic connections, the sleep–wake cycle, and cortical fragmentation.

(2) We introduce different neuroimaging methods of anesthesia, including functional magnetic resonance imaging (fMRI), positron emission tomography (PET), functional near-infrared spectroscopy (fNIRS), and EEG. Furthermore, we summarize the advantages and disadvantages of these techniques.

(3) We analyze the shortcomings of the current electrophysiological anesthesia-monitoring methods in clinical use and compare them with the methods used in basic research. We also introduce the theory of brain connectivity and graph theoretical analysis, with a focus on the role and importance of this conceptual framework in anesthesia research. There has been a focus on discovering the brain connectivity and networks in anesthesia over the past five years; furthermore, based on the literature from this period, we discuss the potential combination of these techniques in clinical and research applications and the potential improvement of monitoring systems.

(4) We propose that low- and medium-density EEG can optimize current clinical anesthesia monitoring methods. Moreover, the combination of small-scale network structure analysis and FC analysis provides a potential opportunity for clinical applications. It is hoped that medium-density EEG will expand the clinical monitoring of responses to different anesthetics and resolve the issue of individual differences in anesthesia monitoring. Furthermore, if medium-density EEG is used in the study of noxious stimuli under anesthesia, it may be possible to monitor the analgesic effects of narcotic drugs during noxious stimulation. Finally, we suggest future directions for dynamic FC and machine learning to help open new avenues for identifying underlying consciousness states under anesthesia.

## 2. Neuroimaging studies of anesthesia

In July 2021, we conducted a literature survey of neuroimaging studies of anesthesia in the Web of Science database using different keyword combinations (Fig. 1). In this section, we briefly introduce the neuroimaging studies of anesthesia. Given that most anesthesia studies were conducted using EEG techniques, the current review focuses mainly on EEG studies of anesthesia and consciousness in Section 3. Moreover, recent findings of anesthesia studies using EEG- and fMRI-based brain network methods are presented in Section 4, considering that most brain network studies were performed using these two modalities.

### 2.1. Functional magnetic resonance imaging

fMRI detects hemodynamic changes caused by neuronal activity, with moderate temporal resolution (i.e., at the second scale) and high spatial resolution (i.e., at the millimeter scale). Because of its high spatial resolution, fMRI has been widely used in the study of spatial activity patterns in the brain, especially in the default mode network (DMN), which exhibits high activity and metabolism [28]. fMRI has also been widely used in anesthesia studies. Many studies have explored the effects of anesthetics on brain activation during stimulation (e.g., tactile, auditory, and visual stimuli). Kerssens et al. [29] studied six male volunteers breathing sevoflurane via a laryngeal mask for a set end-tidal concentration. They tested the volunteers' memories after recovery and imaged the fMRI responses to auditory stimulation. The results showed that sevoflurane induced the dose-dependent suppression of auditory blood oxygen level-dependent signals, which likely limited the word processing during anesthesia and compromised memory. Dueck et al. [30] used fMRI to monitor responses to auditory stimulation under propofol anesthesia and found that the ability to process auditory information decreased in a dose-dependent manner; however, primary cortical responses to sound were intact; a response was still observable following auditory stimulation under general anesthesia. Plourde et al. [31] observed the same result and found that the cortical areas involved in language and vocabulary were inhibited under anesthesia. Lower-level cortical responses of the auditory cortex were preserved under anesthesia, whereas higher-level cortical responses were absent. There have also been accumulating studies on visual stimulation under anesthesia. Ramani et al. [32] studied visual stimulation under sevoflurane at 0.25 MAC and found that this anesthetic affected the primary visual cortex and certain higher-order association cortices. In studies of brain activation under different stimulation

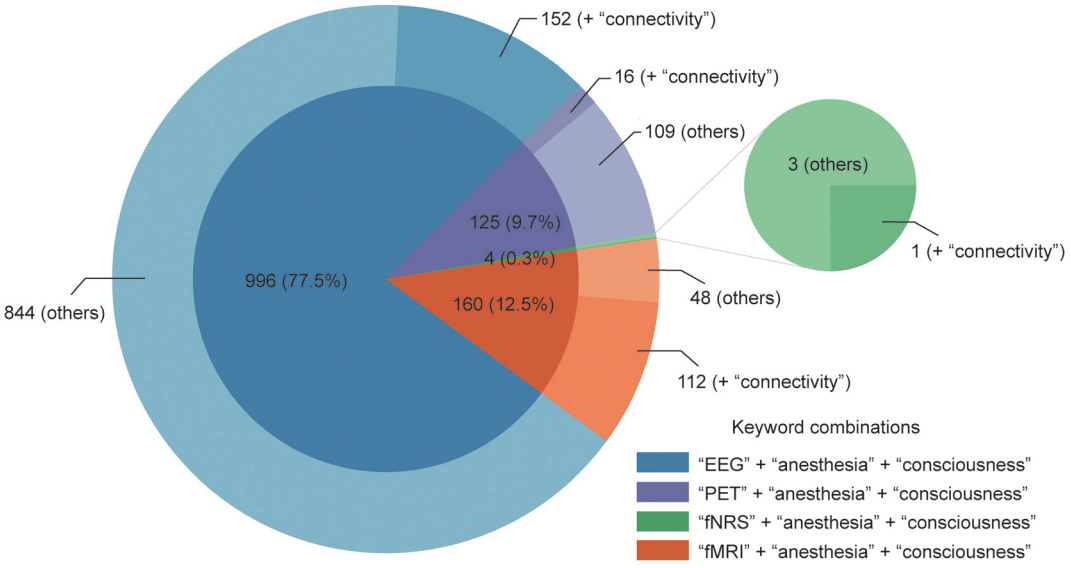


**Fig. 1.** Neuroimaging studies of anesthesia in the Web of Science database searched in July 2021. The pie chart in the center are the number and percentage of neuroimaging studies of anesthesia that are categorized according to different imaging methods (i.e., EEG, fMRI, PET, and fNIRS). The circular diagram stands for the number of brain network studies (added with the keyword "connectivity") and other studies of anesthesia.

conditions, it has been shown that stimulus- and task-related activity in this state affects not only regional activities but also FC (including interhemispheric connectivity) [33]. Specific brain network configurations are necessary for awareness [34]. Anesthetic drugs preferentially act on higher-order rather than lower-order connections [35–37]. Peltier et al. [38] found that sevoflurane affected the temporal synchrony of the motor cortex in a dose-dependent manner, and a transition from bilateral to unilateral FC was also observed in the network.

### 2.2. Positron emission tomography

PET is widely used in brain imaging and brain metabolism research. PET exploits the annihilation of negative electrons and emitted positrons from isotope decay, detecting gamma rays generated by annihilation events after compounds labeled with positron-emitting isotopes are injected into the human body. As a result, the distribution of radionuclides in the human body can be traced, enabling three-dimensional tomography. PET is often used to measure changes in regional cerebral metabolic rate (rCMR) and regional cerebral blood flow (rCBF) to reflect changes in brain function. In 1995, Alkire et al. [39] used PET to study human brain metabolism during anesthesia for the first time. Six volunteers underwent two PET scans each, with one scan assessing conscious baseline metabolism, and the other scan assessed metabolism when the volunteers were unresponsive. The whole-brain metabolic rate was found to decrease during anesthesia compared to wakefulness. The decrease in the metabolic rate varied in different brain regions. In the following studies, Alkire et al. [40,41] used PET to study the effects of different drugs on brain metabolism while further studying thalamic metabolism [8] and proposed a thalamocortical connection model. Since then, several studies have been published, for example, Fiset et al. [35] used PET to scan global cerebral blood flow (CBF) and rCBF during propofol anesthesia and found that thalamic metabolism and blood flow during anesthesia decreased with increasing anesthetic concentrations. Synergistic changes between thalamic and midbrain blood flow confirmed the connectivity between these two regions. This result supports the hypothesis that narcotics induce concentration-dependent effects on specific neuronal networks rather than a non-specific, generalized effect on the brain. Bonhomme et al. [42] also studied the supply of blood to the thalamus and cortex under vibratory stimulation during anesthesia. In the awake state, vibratory stimulation caused an increase in CBF in the left thalamus and parts of the cortex, whereas under propofol anesthesia, changes in the thalamus, parietal lobe, and prefrontal cortex were reduced in a concentration-dependent manner. The effect of propofol on vibratory stimulation first appeared in the somatosensory cortex and then in the thalamic region.

### 2.3. Functional near-infrared spectroscopy

fNIRS uses near-infrared light to irradiate one or more tissues and collects the reflected light for further analysis. It can measure cerebral hemodynamic response. Compared to fMRI, the advantages of low cost, portability, relatively high temporal resolution, and capability of long-term recording make fNIRS an increasingly popular neuroimaging technique for brain function research in recent years, especially in resting-state brain studies. In contrast to other methods for anesthesia monitoring, near-infrared spectroscopy (NIRS) can monitor changes in circulatory oxygenation in the cerebral cortex, which can reflect tissue oxygen consumption. Owen-Reece et al. [43] compared the hemodynamics between awake and anesthetized patients using NIRS and concluded that NIRS has the potential to distinguish between an awake state and an anesthetized state. Lovell et al. [44] organized 36 healthy patients who were randomly allocated to undergo anesthesia induction with etomidate, propofol, or thiopental. Dose-dependent changes in CBF were observed for each anesthetic. Curtin et al. [45] found that changes in oxygenated hemoglobin ($HbO_2$) in the dorsolateral prefrontal cortex were correlated with changes in propofol. Although fNIRS showed a concentration-dependent change in some anesthetics, studies have reported that midazolam, aminophylline, and isoflurane may affect the DOA despite having no effect on oxygen saturation [46]. One of the widespread uses of fNIRS is to detect resting-state FC and describe the topological network of the brain. However, few studies to date have used fNIRS to study FC associated with anesthesia. There is no doubt that these studies offer evidence for the capacity of fNIRS to aid in the assessment of anesthetic depth.

### 2.4. Electroencephalography

EEG has always been essential in neuroimaging studies of the brain in various cognitive/mental states. During anesthesia, the changes in various frequency bands in the EEG are correlated with the concentration of the anesthetic agent. In previous studies of the neural mechanism underlying anesthesia, high-density EEG was commonly used to monitor regional changes in the cerebral cortex under different anesthesia conditions, while single- or dual-channel EEG is mainly used in clinical applications for anesthesia monitoring. In fact, single- or dual-channel EEG and the corresponding calculated indicators have been widely used in clinics. However, it has been found that single-channel EEG has a significant limitation in monitoring anesthesia [47–49]. Given that most of the anesthesia studies were performed using EEG techniques, a detailed review of EEG studies of anesthesia and consciousness is provided in Section 3.

### 2.5. Brief summary

In summary, the widely used neuroimaging techniques for anesthesia studies include fMRI, PET, fNIRS, and EEG. The characteristics of these techniques are summarized in Table 1. Heuristically, fMRI and fNIRS detect hemodynamic responses related to neuronal behavior, while fNIRS can detect changes in both oxyhemoglobin and deoxyhemoglobin related to neuronal behavior. PET can measure changes in the rCMR and regional CBF, which can also uniquely reflect molecular metabolism. EEG is a general reflection of electrophysiological brain activity. Due to the apparent limitations imposed by the large size of the equipment, PET and fMRI are unsuitable for long-term clinical monitoring, especially during surgery. EEG and fNIRS, however, are more portable and can be combined with other clinical monitoring equipment, giving them great promise for clinical studies.

## 3. EEG studies of anesthesia and consciousness

### 3.1. Low-density EEG in traditional clinical studies

The bispectral index (BIS) (Fig. 2) has been used to analyze the frequency and power of EEG signals [50]. The BIS mostly monitors changes in EEG signals in the prefrontal region and results in a normalized index of 0–100. Researchers have compared the MAC and BIS in anesthesia monitoring with a large number of patients and concluded that both are prone to intraoperative awareness in the process of anesthesia monitoring and that there was no substantial difference in this effect across measures [51]. Notably, the BIS in the same state of consciousness tended to decrease with increasing age [52–55]. The BIS also varies greatly with different drugs, which suggests a lack of practicability for accurate monitoring of anesthesia when multiple drugs are used in combination [47–49].

**Table 1**
Characteristics of neuroimaging techniques in anesthesia studies.

| Feature | PET | fMRI | fNIRS | EEG |
|---|---|---|---|---|
| Temporal resolution | Low | Low | Moderate | High |
| Spatial resolution | High | High | Moderate | Low |
| Measuring | Molecular metabolism | Blood oxygen level-dependent response | Blood oxygen level-dependent response and hemoglobin (Hb) | Neural electrical activity |
| Cost | Expensive | Expensive | Accessible to many researchers | Accessible to many researchers |
| Portability | Not portable | Not portable | Portable | Portable |
| Harmfulness | Radiotracer may harm participants | Harmless | Harmless | Harmless |

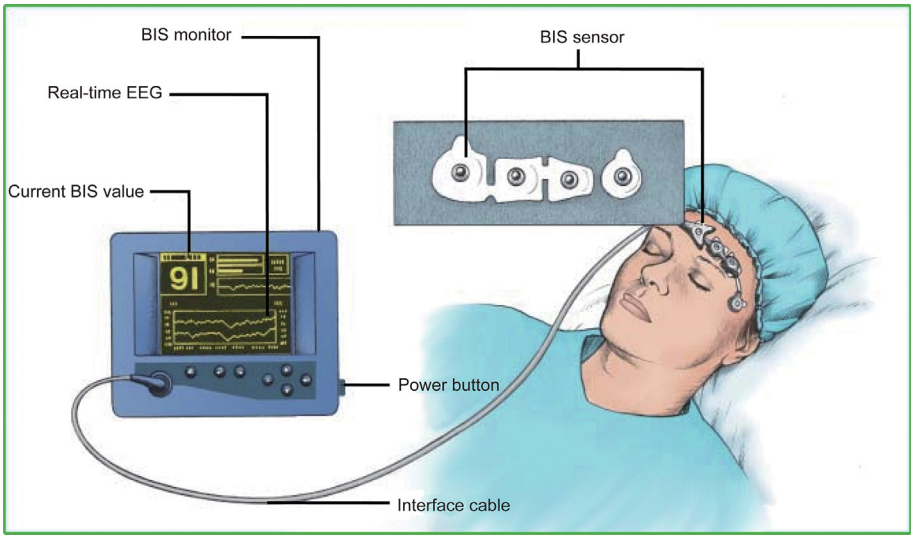


**Fig. 2.** A sketch of BIS measurement. The BIS sensor includes two channels for measurement and two channels for reference. The BIS is normalized as an index ranging from 0 to 100 for interpretation by anesthesiologists. Reproduced from Ref. [50] with permission of Dove Medical Press, ©2018.

Moreover, there was a significant difference in BIS scores across individuals [56].

Entropy is an index used to describe signal uncertainty. The main application of entropy in clinical anesthesia monitoring is the assessment of the M-entropy. The shortcoming of M-entropy is similar to that of BIS in that it reflects only part of the regional EEG and differs markedly depending on the drug used. This index loses effectiveness under certain conditions, such as during burst suppression [57,58].

Time-frequency analysis of EEG data can show changes in the EEG frequency spectrum over time. Purdon et al. [59] found that different EEG signal patterns appear under different anesthetics. Particularly, a single anesthesia index may not be suitable when a combination of drugs is used during anesthesia, but the characteristics of different drugs can be distinguished according to the EEG time–frequency map. This result was consistent with the view of Akeju et al. [60,61], who showed that time–frequency analysis of the EEG power spectrum may be a better indicator for anesthesia monitoring [62].

Intraoperative evoked potential (EP) monitoring was first reported in the late 1970s [63]. Auditory evoked potential (AEP) is the electrophysiological activity triggered by a sound stimulus in auditory pathways that reaches the primary auditory cortex via ascending auditory pathways originating from the brain stem. Among AEPs, the middle-latency AEP (MLAEP) shows a dose-dependent decrease under most anesthetics; therefore, the MLAEP is particularly suitable as an anesthetic index [64]. Compared with the BIS value, an AEP is a superior reflection of the bistable characteristics of the brain sleep–wake cycle, changing rapidly during the transition from anesthesia to wakefulness [65,66]. However, similar to BIS, AEP shows significant individual differences [67], and recognition of this waveform is complex and vulnerable to external interference [68].

### 3.2. High-density EEG in studies of anesthesia mechanisms

Given that the anesthesia process involves changes in multiple brain regions, there is a growing research interest in utilizing high-density EEG to investigate the neural mechanisms of anesthesia, with the ultimate aim of revealing salient and practicable biomarkers for anesthesia monitoring. Moreover, to fully understand the electrical activity during anesthesia, especially in the cortical and subcortical structures, researchers have recruited patients with Parkinson's disease using electrodes implanted in the brain to observe cortical and subcortical EEG activity under the sole action of either propofol or sevoflurane. They found that consciousness was reflected mainly in the activity of the cortex; however, subcortical structures could better predict the response to a noxious stimulus [21], and intracranial EEG revealed the first signs of recovery from deep anesthesia [69].

Alkire et al. [18] used transcranial magnetic stimulation to stimulate the anterior motor cortex and observed mutual transmission of information between brain regions. They concluded that LOC was related to the ability of the cortex to integrate information. When consciousness disappears, the transfer entropy (TE) between the cortical regions decreases. This phenomenon may be a common mechanism of anesthesia-induced unconsciousness and conforms to the cortical fragmentation theory. Furthermore,

researchers have found that LOC is accompanied by a decrease in cortico-cortical connections from the frontal lobe to the parietal lobe [70–72]. The above studies have shown that LOC under anesthesia may be caused by a decrease in the ability to integrate across cortical regions.

Purdon et al. [73] recorded the sound of a mouse click every 4 s as a stimulus. They used high-density EEG (h-EEG) to observe changes in the brain and found that when the propofol concentration was increased, the low-frequency EEG power (< 1 Hz) increased. Meanwhile, the spatial coherence of the occipital alpha oscillation (8–12 Hz) was reduced. However, spatially coherent frontal alpha oscillations increased. Furthermore, the power of the 0.1–1.0 Hz band increased throughout the scalp and forehead, the power of the 8–12 Hz band increased in the forehead, and the power of the 25–35 Hz band mainly increased in the parietal lobe. Huang et al. [74] implanted electrodes into the bilateral anterior cingulate cortex, hypothalamus, periaqueductal gray, and sensory thalamus in patients with chronic pain. The subcortical alpha oscillations increased, whereas subcortical gamma oscillations decreased when the propofol concentration increased. Moreover, subcortical structures also exhibited oscillations similar to those of cortical structures, further indicating that the FC of the alpha oscillation may serve as a marker of consciousness. h-EEG has been widely used to assess brain network changes under anesthesia. It is usually observed that partial rather than overall connectivity is reduced under anesthesia. Propofol has been shown to preferentially reduce FC within the thalamic nuclei in a nonspecific manner. Certain anesthetics can also reduce high-order thalamocortical connectivity [75]. The mechanisms of these brain changes under anesthesia remain to be studied, and high-density EEG may represent a powerful method for such elucidation.

## 4. Brain network studies of anesthesia

### 4.1. Brain network and graph theoretical analysis

The human brain is highly complex in terms of structure and function. Therefore, investigating the functional and structural mechanisms of the brain may benefit from a systematic perspective. A variety of advanced brain imaging and processing techniques have provided some of the first insights into understanding the structure of the brain. Brain network analysis based on brain imaging technology has made it possible to assess whole-brain function. The human brain can be considered a connectome composed of large-scale networks. Many studies have shown that brain networks play an important role in neural communication, information processing, and integration. The rise of network neuroscience has brought new approaches to the multilevel analysis of the brain, exploring the structure, function, and efficiency of the brain from an integrated perspective, and seeking ways to map, record, analyze, and model the elements and interactions of this neurobiological system [76]. Network neuroscience uses various imaging techniques to obtain important information regarding the brain.

#### 4.1.1. Connectivity analysis

Connectivity is the foundation for building brain networks. It evaluates the relationship between different brain nodes and constructs connections between brain regions as the basic edges of the brain network. A diagram of the EEG brain network construction is shown in Fig. 3 [77]. Heuristically, brain connectivity can be divided into three types: ① structural connectivity, the physical connections between brain regions (typically corresponds to white matter fiber tracts between pairs of brain regions); ② FC, the temporal dependency between the activities of spatially distant brain regions (that is usually estimated from fMRI and EEG data); and ③ effective connectivity, the direct or indirect causal influences of one brain region on another (that has been widely employed in EEG signal analyses) [78,79]. By combining graph theory with connectivity analysis, we can understand changes (both static and dynamic) in the rich topology of the brain, which is critical in the evolution of anesthesia studies. Connectivity methods can be applied not only to original EEG signals but also to broad or narrow bands within the original signals, such as delta (1–4 Hz), theta (4–7 Hz), alpha (8–12 Hz), beta (13–30 Hz), and gamma (30–100 Hz). In Table 2 [80–98], we provide a brief introduction of several widely used methods for connectivity estimation. A more detailed description of connectivity estimation and their interpretation can be found in reviews of this topic [99–101].

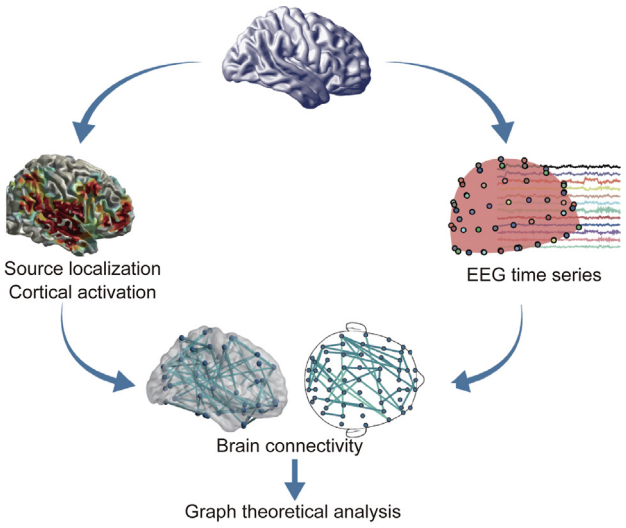


**Fig. 3.** The construction of an EEG-based brain network. An adjacency matrix (which can describe brain connectivity) was constructed through the relationship (computed by connectivity estimation methods) between the time series at sensor space or the time series at source space after source localization. Source localization is a method to estimate the location, direction, and intensity of the source neural activity in the brain according to the electrical signals measured at the scalp [77].

#### 4.1.2. Graph theoretical analysis

In 1736, the Swiss mathematician Leonhard Euler introduced the famous "Seven Bridges of Konigsberg" problem. This problem introduced graph theory to mathematics as a new branch that has been prosperous ever since. Heuristically, graph theory is a mathematical analysis framework for the quantitative assessment of the topological architecture of a network. A paper published in *Nature* in 1998 [102] found that the neural network of the nematode *Caenorhabditis elegans* exhibited characteristics of a small-world network. This influential paper led to the renaissance of network sine for investigating the topology of a wide variety of complex systems in various areas, including neuroscience, social science, communication, physics, biology, and computer science. In fact, many complex systems show remarkably similar macroscopic behavior, despite profound differences in the microscopic details of the elements of each system or their mechanisms of interaction.

Most recently, graph theory has become an important analytic method for studying complex networks in the field of neuroscience, and it is considered to be an important tool for describing the characteristics of brain networks. Convergent evidence has demonstrated that the brain is a small-world network characterized by a larger cluster coefficient and smaller characteristic path length than a random network. The small-world characteristics

**Table 2**
Methods for connectivity estimation.

| Type | Properties | Formulas | Measurement and meaning | References |
|---|---|---|---|---|
| Undirected connectivity | Coherence (COH) | $\mathrm{COH}_{XY}(\omega)=\frac{\lvert S_{XY}(\omega)\rvert}{\sqrt{S_{XX}(\omega)S_{YY}(\omega)}}$ | $\mathrm{COH}_{XY}(\omega)$ measures the correlation between signal $X$ and $Y$ at frequency $\omega$; $S_{XY}(\omega)$ is the cross-spectral density; and $S_{XX}(\omega)$ and $S_{YY}(\omega)$ are the auto spectral densities of signal $x$ and $y$, respectively. | [80] |
| | Phase lag index (PLI) | $\mathrm{PLI}=\frac{1}{N}\left\lvert\sum_{t=1}^{N}\mathrm{sign}(\Delta\phi_t)\right\rvert$ | The PLI is the measurement used for measuring phase synchrony; sign() denotes the sign function; $\Delta\phi_t$ is the phase difference at time $t$; and $N$ is the number of samples. | [81] |
| | Weighted PLI (wPLI) | $\mathrm{wPLI}=\frac{\lvert E\{\lvert\Im(Z)\rvert\mathrm{sign}[\Im(Z)]\}\rvert}{E\{\lvert\Im(Z)\rvert\}}$ | The wPLI is the degree of phase synchronization; $Z$ is the cross-spectrum; $\Im()$ denotes the imaginary component; and $E\{\}$ is the expected value operator. wPLI is a derivative of PLI. | [82] |
| | Phase locking value (PLV) | $\mathrm{PLV}=\frac{1}{N}\left\lvert\sum_{t=1}^{N}e^{j\Delta\phi_t}\right\rvert$ | The PLV estimates the phasic interrelation between two signals; $e$ is the Euler constant; and $j$ is the imaginary unit. The imaginary part of PLV (iPLV) and the corrected imaginary part of PLV (ciPLV) are derivatives of PLV. | [83,84] |
| | Phase lag entropy (PLE) | $\mathrm{PLE}=-\frac{1}{\lg(2^m)}\sum_j p_j\lg p_j$ | PLE incorporates the temporal dynamics of the instantaneous phase time series into the phase synchronization analysis; $m$ represents pattern size (word length); and $p_j$ is the probability of the $j$th pattern. | [85] |
| | Pairwise phase consistency (PPC) | $\mathrm{PPC}=\frac{2}{N(N-1)}\sum_{j=1}^{N-1}\sum_{k=(j+1)}^{N}f(\theta_j,\theta_k)$ | PPC is a measure that quantifies the distribution of phase differences across observations, where $f(\theta_j,\theta_k)=(\cos(\theta_j)\cos(\theta_k)+\sin(\theta_j)\sin(\theta_k))$. $\theta_j$ and $\theta_k$ are the relative phases from two observations. | [86] |
| | Phase-slope index (PSI) | $\mathrm{PSI}=\Im\left(\sum_{f\in F}C_{ij}^{*}(f)C_{ij}(f+\delta f)\right)$ | The PSI is a generic quantity to infer dominant undirected interactions, where $C_{ij}(f)=S_{ij}(f)\Big/\sqrt{S_{ii}(f)S_{jj}(f)}$ is the complex coherency; $S$ is the cross-spectral matrix; $\delta f$ is the frequency resolution; and $F$ is the set of frequencies over which the slope is summed. $*$ denotes the transpose and complex conjugate operation. | [87] |
| | Orthogonalized amplitude envelope correlation (orthAEC) | $\mathrm{orthAEC}(t,f)=\Im\left(y(t,f)\frac{x'(t,f)}{\lvert x(t,f)\rvert}\right)$ | The variable orthAEC measures synchronization between signal envelopes. The complex signals $x$ and $y$ are functions of time $t$ and frequency $f$; $x'$ is the complex conjugate of $x$. | [88] |
| | Mutual information (MI) | $\mathrm{MI}(X;Y)=\sum_{x,y}p(x,y)\ln\frac{p(x,y)}{p(x)p(y)}$ | MI is the measurement of information shared by both the $X$ and $Y$ signals; $p(x,y)$ is the joint distribution of $X$ and $Y$; and $p(x)$ and $p(y)$ are the marginal distributions of $X$ and $Y$, respectively. | [89] |
| | Partial MI (PMI) | $\mathrm{PMI}(X,Y\lvert Z)=\mathrm{SDE}(X,Z)+\mathrm{SDE}(Z,Y)-\mathrm{SDE}(Z)-\mathrm{SDE}(X,Z,Y)$ | PMI measures the amount of information shared by $X$ and $Y$ while discounting the possibility that $Z$ drives both $X$ and $Y$; and SDE denotes the Shannon differential entropy. | [90] |
| Directed connectivity | Phase TE (PTE) | $\mathrm{PTE}_{X\to Y}=\mathrm{SE}[\theta_y(t),\theta_y(t')]+\mathrm{SE}[\theta_y(t'),\theta_x(t')]-\mathrm{SE}[\theta_y(t')]-\mathrm{SE}[\theta_y(t),\theta_y(t'),\theta_x(t')]$ | PTE is a measure of directed connectivity between phase time series; $\theta_x(t)$ and $\theta_y(t)$ are the past phases of $X$ and $Y$ at time $t$, respectively; and SE is Shannon entropy. | [91] |
| | Partial directed coherence (PDC) | $\mathrm{PDC}_{ij}(f)=\frac{A_{ij}(f)}{\sqrt{a_j^{*}(f)a_j(f)}}$ | PDC describes the relationships between the present time series of $x_i(n)$ and the past of $x_j(n)$; $a_j(f)$and $A_{ij}(f)$ come from the prediction error covariance matrix associated with multichannel autoregressive (AR) models. The generalized PDC and renormalized PDC are derivatives of PDC. | [92–94] |
| | Directed transfer function (DTF) | $\mathrm{DTF}_{ij}(f)=\frac{H_{ij}(f)}{\sqrt{h_j^{*}(f)h_j(f)}}$ | The DTF is defined similarly to PDC. The DTF uses the elements of the transfer function matrix $H_{ij}(f)$, whereas PDC uses those of $A_{ij}(f)$. $h_j(f)$ is the column of the inverse of the transfer function matrix. The direct dDTF is a derivative of the DTF. | [95,96] |
| | Directed phase–amplitude coupling (DPAC) | $\mathrm{DPAC}=\frac{1}{\sqrt{N}}\frac{\lvert\sum_{t=1}^{N}a(t)e^{j\phi_t}\rvert}{\sqrt{\sum_{t=1}^{N}a(t)^2}}$ | DPAC is the measurement used to measure coupling of phase and amplitude, where $a$ is the amplitude and $\phi_t$ is the phase. | [97] |
| | Granger causality (GC) | $\mathrm{GC}_{y\to x}=\ln\left(\frac{V_{x\lvert x}}{V_{x\lvert x,y}}\right)$ | $\mathrm{GC}_{y\to x}$ is the GC from $y$ to $x$ (predicting $x$ from $y$), where $V$ is the variance of the residuals, which is estimated using AR models. | [98] |

$N$, $t$, $e$, $j$, $*$, sign(), $\Im()$, and $\Delta\phi_t$ share the same meaning across the formulas in this table.

of human brain networks indicate that brain networks are organized in a particular pattern to maintain a balance between local segregation and global integration. That is, lower-level information can be processed locally and modularly, whereas higher-level information requires the integration of different functions distributed over the brain.

Here, we provide a brief introduction to several widely used graph theoretical analysis (Table 3). In Fig. 4, we provide a schematic diagram of several representative topological properties in the graph theoretical analysis. A more detailed description of the graph theoretical parameters and their mathematical formulations can be found in the reviews of the topic [103–105]. Open software toolboxes for graph theoretical analysis are available for those who are interested in practice [106–113]. It should be mentioned that the estimation of these network measurements should consider network characteristics (i.e., weighted/binary, directed/undirected) into account. According to the characteristics of the network, different mathematical formulas should be adopted.

#### 4.1.3. Dynamic functional connectivity analysis

The brain dynamically integrates, coordinates, and responds to internal and external stimuli across multiple time scales, while the static characteristics described above cannot characterize the dynamic characteristics of brain networks. Given the known dynamics and conditional dependence of brain activity [114], it is natural to expect that FC indicators calculated from fMRI or EEG data will change over time, which implies that measures assuming stationarity over a full resting-state scan may be too simplistic to capture the full extent of resting-state activity [115]. In fact, dynamic FC (dFC) analysis is considered to be a more efficient way to uncover specific functional integration properties under various states [116]. Recently, several groups have presented thorough reviews pertaining to the methodological aspects and perspectives of dFC analysis [117–119]. Here, we would briefly introduce the basic concept of dFC analysis; for researchers who are interested in using dFC analysis, they could refer to the reviews.

Unlike static FC analysis, where brain networks were constructed in a fixed window, that is, an FC network was typically estimated during the whole scan period of several minutes in most resting-state fMRI network studies [120], dFC constructed a network in a temporal manner. The most widely used analytical strategy for investigating dFC consists of segmenting the time courses from spatial locations (brain voxels or regions) into a set of temporal windows, inside which their pairwise connectivity is probed, which is called the sliding-window approach. This process divides the entire scan time series into a windowed segment series. Given a sufficient number of data points for robust calculations, any metric that can be applied to the entire scan can, in principle, be used for sliding window analysis. The results of hard clustering (or fuzzy clustering, *K*-means clustering, principal component analysis, etc.) on dFC estimates can be used to calculate group-wise state measures and conduct statistical analysis. Finally, the temporal properties of dFC states and the topologies of dFC states (modularity, efficiency, etc.) were evaluated [117,119,121]. In Fig. 5, we provide a schematic diagram of the analysis framework for the dFC.

**Table 3**
Description of topological measures in graph theoretical analysis.

| Property type | Properties | Measurement and meaning |
|---|---|---|
| Global properties | Clustering coefficient ($C$) | The $C$ is the ratio of the actual number of edges among all neighbor nodes directly connected to a node. A higher $C$ indicates a more segregated network topology. |
| | Characteristic path length ($L$) | $L$ represents the average value of the shortest path among all node pairs. A lower $L$ indicates high efficiency of parallel information transfer of a network. |
| | Small-worldness ($\sigma$) | $\sigma$ is an integrated indicator, greater values of which represent a shorter feature path length and a larger $C$. A value greater than 1 typically indicates a small-world network. |
| | Global efficiency ($E_{glob}$) | $E_{glob}$ measures network efficiency for parallel information transmission and is inversely proportional to $L$. |
| | Local efficiency ($E_{loc}$) | $E_{loc}$ means the efficiency of local connections between arbitrary nodes; this property is defined as the average of the $E_{glob}$ of adjacent subgraphs of node $i$. |
| | Modularity ($Q$) | $Q$ refers to the optimal division of a brain network into smaller communities, where the connections within the modules are dense and the connections between modules are sparse. |
| | Assortativity | Assortativity measures the correlation between the degree of a node and the mean degree of its nearest neighbors. |
| | Hierarchy ($\beta$) | $\beta$ quantifies the power-law relationship between the $C$ and degree $N$ of the nodes. |
| | Rich clubs | Rich clubs are elite "cliques" of high-degree network hubs that are connected topologically with high efficiency. |
| | Transitivity | Transitivity is the fraction of all possible triangles present in a network. |
| | Synchronization | Synchronization measures the propensity of all nodes to fluctuate in the same wave pattern. |
| Nodal properties | Node degree ($N_{degree}$) | $N_{degree}$ is the number of connections joining a node to the rest of the network. |
| | Node strength ($N_{str}$) | $N_{str}$ is the sum of edge weights that link a node to the other nodes in a weighted network. |
| | Betweenness centrality (BC) | BC is defined as the number of shortest paths between other node pairs passing through the node. |
| | Nodal efficiency ($E_{nodal}$) | $E_{nodal}$ is defined as the reciprocal of the harmonic mean of the shortest path length between a node and all other nodes. |
| | Closeness centrality (CC) | CC quantifies how quickly a given node in a connected graph can access all other nodes; the more central a node is, the closer it is to all other nodes. |
| | Eigenvector centrality (EC) | EC of node $i$ is equivalent to the $i$th element in the eigenvector corresponding to the largest eigenvalue of the adjacency matrix. |
| | Participation coefficient | The participation coefficient of a node quantifies the distribution of its connections among separate modules. |
| | PageRank centrality | PageRank centrality is a variant of EC. PageRank is defined as the stationary distribution achieved by instantiating a Markov chain on a graph. The PageRank centrality of a node is proportional to the number of steps spent at the node as a result of such a process. |
| | $k$-coreness centrality | The $k$-core is the largest subgraph comprising nodes whose degree is at least $k$. The $k$-coreness of a node is $k$ if the node belongs to the $k$-core but not to the $(k + 1)$-core. |
| | Network cost | Network cost is the ratio of the existing number of edges to the total number of possible edges in the network. |

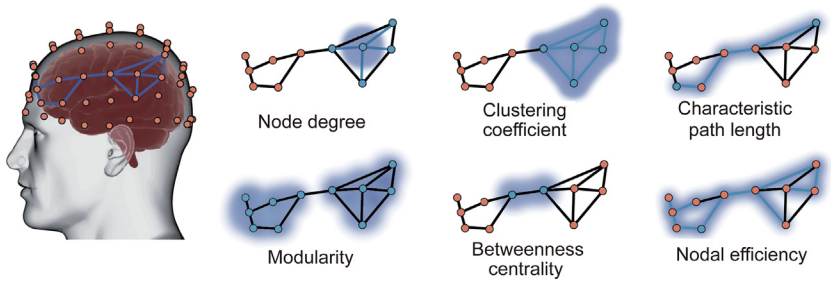


**Fig. 4.** Schematic diagram of several representative topological properties in graph theoretical analysis. The detailed descriptions and the formulas for graph theoretical analysis estimation were presented in Table 3.

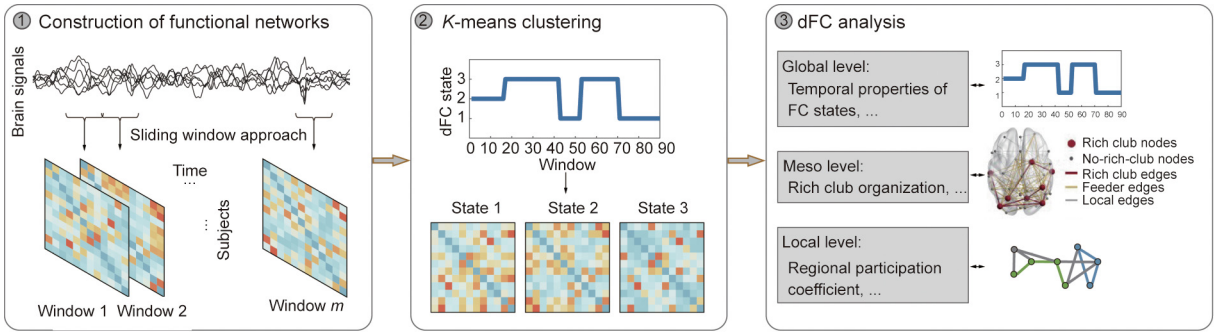


**Fig. 5.** Schematic diagram of analysis framework for dFC construction and quantitative assessments. Step 1: construct the time-varying functional networks using the sliding window approach; step 2: identify the dFC states using *K*-means clustering, conduct the statistical analysis; step 3: perform the dFC analysis at global, meso, and local level as needed.

### *4.2. Actual anesthesia studies using brain networks*

With the development of brain network analytic technologies in the field of neuroscience, an increasing number of scientists have used graph theoretical analysis to investigate state changes of consciousness under anesthesia, coinciding with the current conceptualization of anesthesia: the common cause of anesthesia-induced unconsciousness is persistent inhibition of the lateral frontal lobe or functional disconnection of the cortex [122]. Hence, we focused on brain network studies on anesthesia. Given that most of these studies were performed using EEG and fMRI, we separated the main findings accordingly.

#### *4.2.1. Anesthesia studies using EEG-based brain networks*

Among the 152 EEG-based articles (Fig. 1), 98 were published in the last five years. The search results were mixed with articles that were not directly related, such as including other neuroimaging methods, analysis of EEG power spectrum, and brain injury studies. Hence, articles that were not directly related to brain connectivity and network analysis, consciousness, or anesthesia were further excluded through manual verification, leading to the final 33 articles that met the inclusion criteria. Most of the included articles were methodological studies, and a few described indications for clinical applications. After screening these articles, we focused on anesthesia and consciousness research using the EEG brain network approach and selected 27 representative articles (Table 4 [85,123–148]). Based on the different principles of FC analysis, we divided these studies into three categories: spectral-based FC, entropy/complexity-based FC, and dFC.

Spectral-based FC: EEG has the advantage of providing spectral information; hence, most of the FC indices were estimated in the spectral domain. Using weighted phase lag index (wPLI) and network analysis, Chennu et al. [123] found that participants with weaker alpha-band networks were more likely to become unresponsive under the same sedation protocol; Kim et al. [124] discussed the functional and topological conditions for explosive synchronization developed in human brain networks, and Lee et al. [125] found that the local connectivity in the delta frequency range increased in the parietal lobe. The wPLI is widely used in functional network studies of anesthesia [130,131,148]. Furthermore, using the basic version of wPLI, Blain-Moraes et al. [129] found that the phase lag index (PLI) did not distinguish between states of consciousness or stages of recovery; Numan et al. [139] reported that the PLI reflected the differences in sedation between midazolam and propofol. Many studies have analyzed coherence and its derivatives [136,137,146]. Furthermore, dynamic casual modeling-based methods, including Granger causality (GC), have been used in anesthesia studies [127,133,144]. As an extension of spectral-based FC at fixed frequency bands, cross-frequency coupling reflects complex interactions between different frequency bands [148–151]. In different tasks, one band of EEG has been shown to modulate other EEG bands [152], and this modulation includes amplitude–amplitude coupling [148], phase–amplitude coupling (PAC) [149–151], and phase–phase coupling [149,150]. This coupling can occur at different frequencies in the same cortex and across different cortical areas [153].

Entropy/complexity-based FC: Entropy and complexity measures of EEG can be used to evaluate information transfer in the cortex. Lee et al. [85] introduced a new metric, phase lag entropy (PLE), to calculate the diversity of time modes of phase relations using the concept of entropy. Unlike traditional phase synchronization methods, which focus on the strength of connectivity, the proposed method reflects whether a given interaction between two signals contains different or fixed connectivity modes. Thus, PLE better reflects the time-varying dynamics of phase relations embedded in neural communication. The results showed that PLE provided better performance in the classification of states of consciousness than did the PLI, a classical time-averaged connectivity

**Table 4**
Summary of EEG network studies on anesthesia in the last five years.

| Time | Drugs | Regions | Index | Channels | Findings | Reference |
|---|---|---|---|---|---|---|
| 2016 | Propofol | Channels on the neck, cheeks, and forehead were excluded | DPAC, wPLI | 91 | Participants with weaker alpha-band networks were more likely to become unresponsive under the same sedation protocol. | [123] |
| 2016 | Sevoflurane | — | wPLI, $E_{glob}$, $N_{degree}$ | 64 | This study demonstrates for the first time that the network conditions for explosive synchronization, formerly shown in generic networks only, are present in empirically derived functional brain networks. | [124] |
| 2017 | Propofol | Frontal and parietal | wPLI, $E_{loc}$ | 27 | Delta power increased from responsiveness to unresponsiveness, and the delta waves shifted from frontal to parietal regions.<br>The local connectivity in the delta frequency range increased in the parietal lobe. | [125] |
| 2017 | Propofol | 10–20 system | PLI, PLE | 12 | PLE outperforms the PLI in classifying states of consciousness. | [85] |
| 2017 | Sevoflurane, isoflurane, midazolam | 10–20 system | PLI, PTE | 17 | Participants recovering from anesthesia had a more integrated network in the delta band than did participants without anesthesia.<br>Patients with hypoactive delirium showed reduced network integration in the alpha band. | [126] |
| 2017 | Nitrous oxide | Parietal and frontal | GC | 8 | Nitrous oxide led to a decrease in connectivity from parietal to frontal regions but no change in the opposite direction.<br>The changes in parieto-frontal connectivity were prominent in the theta, alpha, and beta frequency bands. | [127] |
| 2017 | Propofol | Frontoparietal | MI, TE | 7 | TE was more effective than MI in representing the amount of information shared between channels.<br>The maximum ($TE_{max}$), minimum ($TE_{min}$), and mean ($TE_{mean}$) of TE were sensitive to drug concentration. | [128] |
| 2017 | Propofol | DMN | PLI, wPLI, $Q$, $E_{glob}$, $E_{loc}$ | 128 | During recovery, network efficiency and posterior alpha patterns increased.<br>The network clustering coefficient was increased during unconsciousness.<br>The PLI did not distinguish between states of consciousness or stages of recovery. | [129] |
| 2017 | Ketamine | — | wPLI | 128 | Significant changes in the theta band, including power and functional connection enhancements, appeared during ketamine anesthesia. | [130] |
| 2018 | Ketamine, propofol, isoflurane | — | wPLI, $Q$ | 128 | The average integrated information ($\Phi$) and the network modularity ($Q$) of the alpha band reflected states of consciousness. Only $\Phi$ showed significant and consistent changes in all frequency bands. | [131] |
| 2018 | Isoflurane, ketamine | — | PLE, PLI, $N_{degree}$ | 32, 64, 128 | Partial phase locking at criticality shapes the FC and asymmetric anterior-posterior PLE topography of the network, with low (high) PLE for high-degree (low-degree) nodes. | [132] |
| 2018 | Propofol | Occipital, parietal, and frontal | DCM | 6 | Cortical time–frequency spectral responses to transcranial magnetic stimulation (TMS) are perturbed by propofol sedation. In addition, changes in both feedforward and feedback connectivity throughout the cortical hierarchy might be involved in the effect of anesthesia on consciousness. | [133] |
| 2019 | Propofol | Synamps 2/RT system | wPLI | 60 | Five common brain functional network patterns were found across all conscious levels. Functional network patterns were found to be supported by anatomical connections during unconsciousness. | [134] |
| 2019 | Propofol, isoflurane | Electrodes on the lowest parts of the face and head were removed | wPLI | 21 | Cortical connectivity was dynamic during the anesthesia maintenance period and had a higher probability of remaining in the same state than switching to a different state. | [135] |
| 2019 | Propofol | 10–20 system | PDC | 12 | This study showed that the use of directed coherence to assess EEG directional connectivity outperformed the BIS and the auditory middle latency response. | [136] |
| 2019 | Sevoflurane | 10–20 system | Cross-spectral coherence | 33 | It was verified that slow-wave connectivity and brain network integration were decreased during general anesthesia with sevoflurane in infants. | [137] |
| 2019 | Propofol | 10–20 system | MI | 4 | Standardized permutation MI has a faster response to drug concentration, less variability in the awake state and stronger robustness to noise than the BIS. | [138] |
| 2019 | Midazolam, propofol | 10–20 system | PLI | 32 | Although the degree of sedation differed between midazolam and propofol, the changes in power were similar. FC and network topology reflected the differences in sedation between midazolam and propofol. | [139] |
| 2019 | Propofol | — | PLE | 4 | The PLE was used for clinical anesthesia monitoring and compared with the BIS value. It was noted that PLE could be used as an indicator of hypnotic depth for patients sedated with propofol. | [140] |
| 2020 | Propofol | 10–20 system | wPLI | 14 | This study compared the brain FC of the same subjects during sleep and anesthesia and found similar connectivity changes. | [141] |
| 2020 | Propofol | Frontal, parietal, and temporal | MI, $C$, $E_{nodal}$, $L$ | 64 | The genuine permutation cross MI reflected propofol-induced coupling changes measured at a cortical scale. LOC was associated with the distribution of the pattern of information integration. | [142] |
| 2020 | Propofol | 10–20 system | dwPLI | 16 | Dynamic connectivity under anesthesia, especially in the alpha and theta bands, may be an informative indicator for assessing neurophysiological changes with age. | [143] |

(*continued on next page*)

**Table 4** (*continued*)

| Time | Drugs | Regions | Index | Channels | Findings | Reference |
|---|---|---|---|---|---|---|
| 2020 | Propofol | – | GC | 31 | Propofol-induced unresponsiveness is marked by a global decrease in information flow, chiefly in the posterior and medial directions from the lateral frontal and prefrontal brain regions. | [144] |
| 2021 | Etomidate (Wada test) | 10–20 system | dwPLI | 24 | The unilateral injection of an anesthetic into one internal carotid artery/hemisphere caused bilateral changes in EEG. | [145] |
| 2021 | Propofol | 10–20 system | PDC | 19 | Propofol-induced anesthesia caused modifications in the EEG signal, leading to a rebalancing between long- and short-range cortical connections, and had a direct effect on the cardiac system. | [146] |
| 2021 | Propofol | – | dPLI, PAC, NSTE | 64 | Disruption of frontoparietal connectivity is a signature of propofol-induced anesthesia. | [147] |
| 2021 | Propofol | – | AEC, wPLI | 128 | The class of connectivity measure chosen to construct functional brain networks may greatly influence what connectivity alterations are noted across states of consciousness and when these alterations are most apparent. | [148] |

DPAC: directed phase–amplitude coupling; wPLI: weighted phase lag index; $E_{glob}$: global efficiency; $N_{degree}$: node degree; $E_{loc}$: local efficiency; PLE: phase lag entropy; PTE: phase TE; GC: Granger causality; MI: mutual information; *Q*: modularity; PDC: partial directed coherence; DCM: dynamic casual modeling; *C*: clustering coefficient; $E_{nodal}$: nodal efficiency; *L*: characteristic path length; dwPLI: debiased wPLI; dPLI: directed PLI; PAC: phase–amplitude coupling; NSTE: normalized symbolic TE; AEC: amplitude envelope correlation.

method. PLE has been studied further [132,140]. Schreiber [154] proposed an information theoretic measure called TE, which quantifies the statistical coherence between systems evolving over time, which has been widely used in EEG studies to quantify the transfer information between channels. Cha et al. [128] found a high correlation between the TE and the plasma concentration of propofol, which was confirmed from the experimental results of clinical data in 39 subjects. Using normalized symbolic TE (NSTE), a derivative of TE, Zhao et al. [147] found a significant decrease in frontoparietal connectivity during anesthesia, which indicates that disruption of frontoparietal connectivity is a signature of propofol-induced anesthesia. Lobier et al. [91] proposed phase TE (PTE), a new measure of directed connectivity among neuronal oscillations using the concept of entropy, which quantifies the TE between phase time-series extracted from neuronal signals by filtering, for instance. PTE is beginning to be used in anesthesia studies [126]. Moreover, mutual information (MI)-based indices are increasingly being used in anesthesia studies [138,142].

dFC: Several recent studies using EEG data to conduct dFC analysis have explored dynamic brain network characteristics under anesthesia. Zhang et al. [134] found five common brain functional network patterns across all conscious levels using 60-channel EEG data. Li et al. [135] and Vlisides et al. [155] characterized the dFC patterns via *K*-means clustering and Markov chain analysis, respectively, and the dFC patterns indicated that a single measure of FC will likely not be a reliable correlate of surgical and experimental anesthesia. The mechanisms of dFC patterns under anesthesia remain to be studied, and compared to fMRI, dFC analysis using EEG with a higher temporal resolution is more suitable for clinical application of anesthesia.

#### *4.2.2. Anesthesia studies using fMRI-based brain networks*

Among the 112 fMRI-based articles (Fig. 1), 59 were published in the last five years. After screening these articles, we focused on anesthesia and consciousness research using the fMRI brain network approach and selected 16 representative articles [156–171] introduced below.

Due to the high spatial resolution of fMRI, an increasing number of studies in recent years have used fMRI to investigate anesthesia-induced brain FC. Furthermore, FC analysis of brain activity has become a hallmark of lucidity. In low-consciousness states, FC of the brain reflects its anatomical substrates [156,172]. From a holistic point of view, the overall connectivity of brain networks is significantly reduced during the transition from awakening to anesthesia, especially in the parietal and frontal lobes [173]. Additionally, fMRI can reflect the functional relationship between cortical and subcortical structures and can reveal interactions between different cortical regions. Recent studies have shown that ketamine and other anesthetics can directly disrupt the transmission of information [157], while propofol reduces FC in the frontal cortex [158] and sevoflurane mainly acts on the FC between the cortex and the thalamus [159]. Various anesthetics act on different targets and affect regional connectivity [14]. These differential patterns are related to the electrical activity of the anesthetized cerebral cortex, described by Mukamel et al. [151] as fragmented in time and space, which exhibits an interruption in long-distance cortical communication and a reservation in short-distance cortical communication. In contrast, Wu et al. [160] found that although the local coherence in most brain regions was relatively high, it was reduced by the action of drugs (e.g., medetomidine and metoprolol), and isoflurane resulted in a decrease in local coherence in the cingulate cortex. A research [161] showed that cortical networks are significantly affected by LOC during temporal states of high integration, exhibiting reduced functional diversity and compromised informational capacity, whereas thalamocortical functional disconnections emerge during states of higher segregation.

The posterior regions of the brain's DMN exhibit spatial reductions in both functional diversity and integration with the rest of the brain during LOC. These studies illustrate drug-specific differences based on the differential targets and effects of each drug on FC. Different anesthetic methods can produce distinctive FC patterns or a typical resting-state fMRI pattern [162], which also indicates that fMRI network connectivity analyses provide characteristic drug information. Moreover, Huang et al. [163] found that the induction and recovery phases of anesthesia may follow asymmetric neural dynamics.

Some studies have analyzed fMRI data from the perspective of whole-brain network features. Standage et al. [164] found that a higher isoflurane dose was associated with an increase in both the number and isolation of whole-brain modules, as well as an increase in the uncoordinated movement of brain regions between these modules. Luppi et al. [165] showed that dynamic states characterized by high brain integration are especially vulnerable to general anesthesia induced by sevoflurane, exhibiting attenuated complexity and diminished small-world characteristics. Furthermore, higher doses of sevoflurane (3% (in volume) and burst-suppression) also compromise the temporal balance of integration and segregation in the human brain. By studying resting-state FC under varying depths of isoflurane-induced anesthesia in nonhuman primates, Areshenkoff et al. [166] found that the apparent brain network fragmentation under anesthesia, rather than reflecting an actual change in network structure, can be simply explained as the result of a global reduction in FC. Vatansever et al. [167] found a persistent modular architecture, yet significant reorganization of brain hubs that formed parts of a wider rich-club collective using resting-state fMRI collected from a group of healthy participants under propofol-induced unconsciousness. The results of the study by Wang et al. [168] demonstrated that the rich-club reorganization in functional brain networks is characterized by the switching of rich-club nodes between the high-order cognitive and sensory and motor networks during propofol-induced alteration of consciousness and natural sleep.

Anesthesia studies using dFC analysis based on EEG are still in its infancy, and some researchers have opened up new horizons for anesthesia research using the dFC analysis based on fMRI. Tsurugizawa and Yoshimaru [169] developed a resting-state fMRI protocol to perform awake and anesthetized functional MRI in mice, which demonstrated a shift from frequent broad connections across the cortex, hypothalamus, and auditory-visual cortex to frequent local connections within the cortex only under light anesthesia compared with the awake state. Yin et al. [170] found a negative correlation between nodal entropy for the distribution of dFC patterns and static FC strength in anesthetized monkeys, but not in awake humans. Ma et al. [156] identified several quasi-stable patterns that dynamically recurred from the awake state into anesthetized states using the sliding window method and *K*-means clustering. Golkowski et al. [171] conducted a pooled spatial independent component analysis and *K*-means clustering of resting-state fMRI data obtained from 16 volunteers during propofol and 14 volunteers during sevoflurane general anesthesia, and the results indicated that higher-order brain regions play a crucial role in the generation of specific network patterns.

## 5. Discussion

In recent years, differences in FC between the states of anesthesia and consciousness have mostly been studied using h-EEG and fMRI. Because of the low time resolution, high cost, and radiation-related risk of PET (although it does have a unique nuclide-tracking ability), it is seldom used in network research examining anesthesia and consciousness. Most research has focused on the overall network configurations under anesthesia and the interactions among specific cortical regions, which opens new research avenues for practical anesthesia monitoring in clinical settings. Based on the methodological concepts of graph theoretical analysis and recent findings in network studies of anesthesia, we summarize several potential ideas worth exploring below: ① the influence of EEG channels on anesthesia monitoring, ② accurate monitoring of different anesthetics, ③ individualized anesthesia monitoring, ④ monitoring the analgesic effects of narcotic drugs under noxious stimulation, and ⑤ combination with fNIRS for multimodal monitoring. We have also suggested methodological considerations and directions for future research.

### 5.1. Influence of EEG channels on anesthesia monitoring

A key question that might hinder the wide application of brain network analysis in clinical practice is the potential optimal scheme for EEG electrodes. More specifically, the potential optimal scheme of EEG electrodes contains the determination of the optimal number and position of the electrodes. Considering the apparent limitations and constraints in clinical settings, it is difficult to maintain a balance between the available data and the convenience of the system for anesthesia monitoring in clinical applications. Interestingly, not all channels are required for reliable anesthesia monitoring. Moreover, in terms of convenience and practicability, an excessive number of electrodes can affect patient wearing in a clinical setting. Generally, information between multiple channels in the same area is redundant. For instance, in most EEG-based network studies of anesthesia (Table 4 [85,123–148]), although high-definition EEG (i.e., 64 and 128 channels) was used for data acquisition, the main observations were obtained based on information from a few specific areas. In fact, the optimal location of electrodes that would capture salient anesthesia-related brain activity deserves further investigation. Nevertheless, the different choices of connectivity analysis methods and network sizes make it difficult to compare the results across different network studies of anesthesia. Through a survey of recent studies [174–176], we summarized the characteristics of EEG with different densities (Table 5). Particularly, the optimal setting of the channel number should take objective into consideration; one should not consider Table 5 as a recommendation. Furthermore, we found that the frontal and parietal lobes contributed the most features [42,70–72,173]. These findings conformed with those of another study [177], wherein thought was considered to be constrained automatically by the DMN and deliberately by the frontoparietal network, and modulation was conducted via the salience network. With the recent advances in machine learning methods, several attempts have been made to select channels with the most prominent features [178,179], which may provide an alternative data-driven approach for optimal channel selection and location determination.

### 5.2. Monitoring of different anesthetics

One of the main drawbacks of the existing clinical monitoring equipment for anesthesia is its limited feasibility, that is, it is suitable only for some anesthetics. Among the various anesthesia

**Table 5**
Characteristics of EEG with different densities in anesthesia studies.

| Feature | Low | Medium | High |
|---|---|---|---|
| Number of electrodes | < 25 | 25–64 | > 64 |
| Spatial resolution | Poor | Moderate | Relatively good |
| Cost | Low | Acceptable | Expensive |
| Convenience | High | Low | Low |

The characteristics of different densities are described in relative terms within the technique of EEG, that are independent of other neuroimaging techniques. The numbers of electrodes are summarized according to references [174–176].

monitoring indicators (including the BIS, AEP, entropy, power spectrum analysis, and cerebral state index), only the BIS has undergone comprehensive, large-sample, and multicenter clinical validation [56]. However, even the BIS, which is widely used in the clinic, is useful only under the action of propofol, sevoflurane, and a few other anesthetics. Moreover, the same BIS value cannot represent the same DOA under different anesthetics, and the effects of drugs also induce considerable differences. Even in the presence of anesthetics, such as nitrous oxide and ketamine, the BIS value increases during the unconscious state. In addition, BIS is affected by many factors, such as opioids and muscle relaxants, which limit the effectiveness of BIS in monitoring the combined use of narcotic drugs. Moreover, it has been shown that intravenous fentanyl (2 $\mu g \cdot kg^{-1}$) can significantly reduce the dose of general anesthetics needed to achieve LOC, which indicates that fentanyl can synergistically enhance the inhibition of consciousness by general anesthetics [180]. This finding makes the accurate monitoring of anesthesia impractical via dosage assessment of anesthetics. Moreover, the use of opioids brings great uncertainty to the current clinical anesthesia monitoring. In fact, the modern anesthesia process generally comprises a combination of multiple anesthetics. Currently, there are no clinical indicators that can comprehensively and accurately reflect brain states under different anesthetics. We believe that the development of new methods for accurate anesthesia would be significantly beneficial for a better understanding of the underlying neural mechanisms. For instance, Kim et al. [131] and Kim and Lee [181] proposed a method that estimates the degree of integration of brain information under anesthesia to distinguish different states under anesthesia. They compared changes in brain information integration during anesthesia with different anesthetics, such as ketamine, propofol, and isoflurane, and found that this method could help identify the state of consciousness, thereby providing clinical evidence to show the superiority of network methods in anesthesia monitoring with different anesthetics. In fact, the forehead or a single brain area signal acquisition approach employed in most traditional anesthesia monitoring methods limits the ability to effectively monitor the effects of ketamine. Studies have shown that ketamine and other anesthetics can directly disrupt information transmission between distinct cortical areas [85]. EEG changes in different brain regions may occur under the actions of a variety of drugs, accompanied by alterations in information transfer and changes in brain synergy. The use of EEG network analysis is therefore expected, which may provide novel indicators to improve practical anesthesia monitoring under conditions with complex anesthetics.

### 5.3. Individualized anesthesia monitoring

Another major drawback of the existing anesthesia monitoring system is the lack of sensitivity to account for individual differences in anesthesia monitoring. Heuristically, individual differences may result from considerable differences in drug sensitivities (or responses) among people of the same age, weight, sex, and other basic conditions. Although the anesthesia and operation times are almost the same under conditions of the same age and physical condition, there are obvious differences in the DOA or the recovery time of patients post operation [123]. Particularly, using the same amount of anesthetics, some patients may regain consciousness during the operation, while others may regain consciousness immediately after the operation, with some patients awake even hours after the operation. To aid clinicians in understanding the state of anesthesia, most indicators (including BIS, M-entropy, and AEP) quantify the DOA to 0–100 intuitive values. This numerical value makes it convenient for clinicians to judge the anesthesia status. Nevertheless, there is evidence to show that the incidence of intraoperative awareness increases with the use of BIS for DOA monitoring [182]. This finding reiterates the need to account for individual differences in interpreting BIS values. Otherwise, some patients would experience intraoperative awareness because of inadequacies. While simplifying clinical monitoring, existing anesthesia monitoring ignores the rich information from the whole brain during anesthesia. Therefore, it is difficult to describe the complex process of anesthesia using simple parameters. Recently, Chennu et al. [123] found that monitoring of the brain and consciousness in the clinic was influenced by different individual sensitivities to anesthetics. To solve this problem, they combined the evaluation of h-EEG spectrum connection networks before, during, and after propofol anesthesia with the measurement of blood drug concentrations. They found that participants were more sensitive to drugs when they had a weak alpha-band network without an anesthesia baseline, despite similar levels of blood drug concentrations. According to this study, it is possible for brain networks to predict individual susceptibility to propofol in clinical settings. If this can be applied to the clinic, it may resolve issues regarding individual differences that have confounded anesthesia monitoring over the years.

### 5.4. Monitoring the analgesic effects of narcotic drugs under noxious stimulation

Unlike consciousness studies, general anesthesia in the clinic consists of three factors: sedation, analgesia, and muscle relaxation. When all three factors are in line during general anesthesia, they are indicative of optimal anesthesia. Current clinical anesthesia monitoring is adequate for evaluating the depth of sedation for muscle relaxation, but the evaluation of the DOA on analgesia requires further improvement. Analgesic monitoring under anesthesia is not the same as in traditional pain research. Pain is based on consciousness, and human pain involves subjective feelings. When patients lose consciousness during general anesthesia, pain mainly manifests as a stress response to a noxious stimulus and a series of simultaneous physiological reactions. This type of stress response to a noxious stimulus is usually monitored by hemodynamic parameters, such as blood pressure and heart rate, as well as by eye pupil movement, breathing, sweating, and other indicators. The most obvious method is to observe the physical responses after noxious stimuli are delivered. However, these indices have great individual differences, and their specificities are not strong. Because EEG signals have good temporal specificity and can extract signals with different spectral characteristics, EEG may have great potential in assessing the effects of anesthesia on analgesia. Noxious stimulation has been shown to alter subcortical activity, while the BIS index reflects the electrical activity of the cerebral cortex; hence, the BIS cannot monitor the levels of analgesia and stress [183]. However, other studies have shown that noxious stimuli have an activating effect on the cerebral cortex [184,185]. Cumulatively, the evidence suggests that the physiological basis of the cortical EEG response to noxious stimuli during general anesthesia is complex. Most current anesthesia/analgesia monitoring methods are multimodal to characterize complex brain responses to noxious stimuli. For example, the qNOX index [186] takes different EEG frequency band data and electromyography (EMG) data as inputs into a fuzzy inference neural network, which is trained to return a composite index ranging from 0 to 99 to describe a noxious stimulus by referring to the body movement stimulated by laryngeal mask intubation. Because of the introduction of the EMG signal, qNOX will be affected when neuromuscular blocking agents are used. For monitoring responses to noxious stimuli, rich information within high-density EEG data has great potential. For instance, Hartley et al. [187] proposed and validated an EEG-based monitoring method for infant noxious stimulation. Using principal component analysis to analyze the time window of interest and defined

the EEG template induced by noxious stimulation, they statistically compared the multichannel EEG patterns with the control group. Specifically, a *t*-test was used to calculate each electrode at each time point, indicating significant differences in brain activity induced by noxious and non-noxious stimuli. When the *t* statistic was higher than the 97.5% threshold, only eight electrodes were recorded, where the Cz electrode had the most significant activity. Notably, Hartley et al. [187] aimed to solve the problem in which babies cannot express their pain to doctors, which is similar to the conditions of anesthetized patients being unable to verbally report pain.

### 5.5. Combination with fNIRS for multimodal monitoring

As we have briefly introduced in Section 2, fNIRS can measure the changes in the parameters related to tissue oxygenation and hemoglobin (Hb) and indirectly measure the effect of blood–nerve activity on hemodynamics and oxygen consumption. These characteristics may compliment the single-modal electrophysiological monitoring. It is noteworthy that both EEG and fNIRS signals were recorded to estimate the most widely used BIS. The feasibility of using single-modal fNIRS as an alternative method for anesthesia classification in clinical practice has already been assessed. For instance, Hernandez et al. [188,189] placed a single-channel fNIRS probe on the right side of the forehead and found that there were significant differences in $HbO_2$ and Hb between the patients in the maintenance and recovery period. From the maintenance period to the recovery period, $HbO_2$ and total Hb levels decreased significantly. Then, they used fNIRS-related indicators as features to train a support vector machine (SVM) classifier. Compared to BIS and MAC, the SVM classifier achieved higher sensitivity and specificity. More importantly, they found that the proposed fNIRS–SVM approach could identify patients' awakening earlier before movement. Moreover, the application of multichannel fNIRS may further improve the monitoring of cerebral hemodynamic changes during anesthesia. Liang et al. [190] designed a multichannel fNIRS system specifically for anesthesia and proved its effectiveness for monitoring the DOA. More recently, multimodal EEG–fNIRS has begun to show its feasibility for anesthesia and/or consciousness monitoring. In a recent study, Yeom et al. [191] used EEG–fNIRS to investigate the electrical and hemodynamic responses during sedation using midazolam and propofol. A gradual increase in EEG power at low frequencies (< 15 Hz) at the frontal and parieto-occipital areas and decreasing EEG power at high frequencies (> 15 Hz) were revealed when consciousness was lost, while the spatio–temporal changes were reserved during the recovery of consciousness (ROC) from unconsciousness. These spatio–temporal EEG patterns were independent of the sedatives used. Moreover, sudden phase shifts in fronto-parietal connectivity at the LOC and ROC, together with mild hemodynamic fluctuations, were also observed. It is noteworthy that although both EEG and fNIRS were identified to be relevant to clinical applications, few studies to date have used fNIRS to study the FC and brain network associated with anesthesia (Fig. 1). In contrast, EEG-based FC and network studies have matured; simultaneously, EEG-based anesthesia monitoring has been widely used in clinical practice. Considering that the brain network plays a pivotal role in the studies of anesthesia, we posit that the fNIRS-based brain network may be a future trend for studies of anesthesia, which may serve as a complementary method to provide comprehensive information for anesthesia monitoring. Given that multimodal EEG–fNIRS inherits the advantages of both techniques, including insusceptibility to electromagnetic interference and convenience for wearing of fNIRS, as well as high temporal resolution and flexible configuration of EEG, we believe that EEG–fNIRS combined with advanced brain network analysis would be a promising method for the development of next-generation anesthesia monitoring systems.

### 5.6. Methodological consideration and future directions

In the past decade, research on brain network studies on anesthesia and consciousness has been gaining momentum, which has not only significantly improved our understanding of the complex neural mechanisms underlying anesthesia and consciousness, but also demonstrated great promise in the application of brain networks in various clinical applications. Here, we propose two main future research directions that deserve attention to promote the development of a practical method for accurate and convenient anesthesia monitoring.

EEGs are known to be susceptible to external disturbances. Existing EEG analysis techniques to solve the nonstationary characteristics of EEG and various physiological artifacts (e.g., eye blink, muscle activity, heartbeat, etc.) in a nonclinical environment have gradually become mature [192,193]. However, the complex environment of clinical surgery and requirements for real-time anesthesia monitoring present a great challenge to EEG artifact removal. High electromyographic activity and electric device interference can cause a spuriously increased BIS value [194]. Furthermore, there are few automated methods for removing electromyographic artifacts in real-time monitoring systems. For instance, García-Cossio et al. [195] discomposed EEG into components using canonical correlation analysis to remove electromyographic components. Nevertheless, advances in EEG artifact removal would still be an important research direction in the future. Moreover, the network analysis approach for most EEG network studies of anesthesia was a static network, which did not show the advantage of EEG in terms of high temporal resolution. Specifically, current techniques for measuring the connectivity between neurophysiological signals do not adequately explain the temporal dynamics of synchronous patterns. For instance, phase synchronization methods, including phase lag [81], and phase locking [84], assume stationarity during the measurement process, and the phase synchronization value is estimated by averaging the phase differences over a period of several seconds, thereby ignoring the temporal dynamics within the window. Moreover, the model-based methods (i.e., GC, partial directed coherence (PDC), directed transfer function (DTF), etc.) require a certain length of time series for model construction [144]. There is also no widely accepted method to estimate the PAC [97], in which current methods have relatively poor sensitivity and require long segments of experimental data. Recently, methods based on information theory have attracted considerable attention. Lee et al. [85] introduced PLE, which calculates the diversity of the temporal patterns of the phase relationship. In contrast to the typical methods of phase synchronization, in which the strength of connectivity is of interest, the proposed measure reflects whether a given interaction between two signals consists of diverse or stereotypic connectivity patterns. Thus, PLE better reflects the time-varying dynamics of phase relationships. Samiee and Baillet [196] proposed the time-resolved PAC to estimate the dynamic PAC that can resolve up to one, optimally two cycles of the underlying low-frequency component. As discussed above, high time resolution FC estimation methods have been adopted in anesthesia studies. What needs to be explained is the application of the dFC framework to EEG studies of anesthesia. First, the sliding window technique used in several recent studies [135,155] has some apparent limitations. Conversely, the choice of window length has always been controversial, given that too short a window length increases the risk of introducing spurious fluctuations in the observed dFC, while a window length that is too long would impede the detection of the temporal variations of interest [119].

However, current studies have limitations originating from the use of a typical rectangular window that might increase the sensitivity to outliers in the detection of dFC, as the inclusion/exclusion of instantaneous noisy observations would appear as a sudden change in the dFC time-course [197]. Window optimization approaches adopted in many studies [198–200] should be considered to eliminate the risk of a rectangular window. Second, dynamic graph analysis is a popular avenue for extracting brain network information from the dFC. Conversely, existing anesthesia research has focused on the transition process of brain states and has lost insight into the continuous functional reorganization of the brain with respect to different network features. Furthermore, the application of dFC state extraction (i.e., through *K*-means clustering) for anesthesia monitoring is debatable, given that the state extraction process requires long-time signal sampling. Although dFC analysis has been widely applied in the diagnosis of schizophrenia [201], autism [202], and mild cognitive impairment [203], the high time resolution requirement of real-time monitoring of anesthesia will be a great challenge for the application of dFC. Given that accumulating evidence has suggested that brain networks are dynamically connected, dynamic EEG connectivity analysis that characterizes spontaneous changes in network-level communication on a fine time scale and the corresponding temporal network measures are increasingly needed to unpack the complex neural mechanisms of anesthesia.

Recently, machine learning methods have been widely developed and utilized in the field of brain disease diagnosis. In this work, we limited our primary focus to the studies of consciousness evaluation and did not elaborate on the applications of machine learning in disease diagnosis. For researchers who are interested in using machine learning to diagnose brain diseases, they could refer to the reviews [204–206] and original articles [207–210]. In the field of consciousness evaluation under anesthesia, machine learning methods have been used to discriminate between awake and anesthetized patients in the early 1990s [211,212]. As anesthesia depth indices such as BIS have become increasingly popular, neural networks and other machine learning methods have been used to analyze EEG data to approximate BIS using other EEG characteristics [213]. Recent studies have used artificial intelligence techniques and spectrum analysis to directly analyze EEG signals to estimate the DOA and compared the accuracy of the quadratic discriminant analysis to analyze the EEG power in different frequency bands [214]. For instance, Shalbaf et al. [215] put a combination of features (including beta-index, sample entropy, Shannon permutation entropy, etc.) to a new neurofuzzy classification algorithm, an adaptive neurofuzzy inference system with linguistic hedges, and obtained 92% accuracy. Hashimoto et al. [216] identified and summarized several themes of artificial intelligence applications in anesthesiology and reviewed the application of machine learning to the DOA monitoring, in which over 40 papers related to EEG and machine learning research on anesthesia monitoring were found. Recently, machine learning analysis of EEG connectivity features has been used for anesthesia monitoring. For instance, Lioi et al. [136] used directed coherence as a feature to identify the DOA and compared its performance with that of the conventional BIS index and the auditory middle latency response. They found a superior performance in discriminating wakefulness from anesthesia (i.e., accuracy = 95%) of machine learning analysis of FC features. Using 128-channel EEG recording, Duclos et al. [148] compared an envelope-based measure (i.e., amplitude envelope correlation (AEC)) and a phase-based measure (i.e., wPLI) of FC to classify states of consciousness, in which a machine learning pipeline implemented using scikit-learn in Python was used for classification. The results showed that AEC showed higher overall classification accuracy, particularly for distinguishing anesthetic-induced unconsciousness from baseline (83.7%). It is noteworthy that the combination of machine learning and brain networks for consciousness and anesthesia monitoring is still in its infancy, and novel methods/techniques could be adopted from studies in relevant fields, including disease classification and cognitive state monitoring. In a recent study, Gao et al. [217] reviewed the application of complex networks and deep learning for EEG signal analysis, covering a wide range of applications, including brain–computer interfaces, neurological disorders, and cognitive analysis.

Heuristically, it is necessary to label anesthetic EEG data according to the state of consciousness prior to applying supervised machine learning techniques to anesthesia monitoring. Evaluating the state of consciousness under anesthesia currently relies on subjective scores (i.e., RSS, MAAS, and SAS), which are based on the patient's unresponsiveness to external disturbances [25–27]. Nevertheless, consciousness is a subjective experience that is not necessarily coupled with connectedness or spontaneous responsiveness during anesthesia [24]. We are usually conscious, connected to our environment, and react to it when we are awake. When we fall asleep, our ability to react and connect to our environment decreases, but it is only during early non-rapid eye movement (NREM) sleep (rich in slow-wave activity) that we become unconscious. Consciousness emerges during NREM sleep at night and comes alive during dreams in rapid eye movement sleep, although we remain disconnected from and largely unresponsive to our environment [24]. Unresponsiveness is not equivalent to unconsciousness under anesthesia, which provides the ideal objective of anesthesia sedation: inferring the underlying consciousness level. Alternatively, although the temporal and spectral features generated by current anesthesia monitoring equipment correlate well with the delivered anesthetic concentration, they provide limited insight into the cerebral mechanisms underlying anesthetic unconsciousness [218]. As discussed in Section 1.1, the potential of brain connectivity and network analysis quantifies the global organized behavior of neural circuits and provides insight into the neural mechanisms underlying LOC under anesthesia, which might become the gold standard for evaluating the underlying consciousness level under anesthesia. This leads us to conclude that the brain network plays an irreplaceable role in consciousness level recognition under anesthesia compared with spectral analysis. Combining machine learning with complex networks may be a valuable research direction. The fusion of interpretable features from brain networks and advanced data-driven methods would help open up new avenues for identifying underlying consciousness states under anesthesia.

## 6. Conclusions

Research on anesthesia and consciousness has long been an essential topic in neuroscience. Despite various hypotheses, there is no valid theory to date that is widely accepted. Researchers are committed to using a variety of methods to study the state transfer of brain consciousness under anesthesia. Obviously, the anesthesia process is not solely caused by the suppression of a single brain region. Whole-brain monitoring methods provide rich information, and the analysis of network architecture provides some of the first quantitative insights into the complex neural mechanisms of anesthesia. To date, most clinical indicators and monitoring systems are based on single- or dual-channel EEG to assess the level of consciousness. Nonetheless, accumulating studies have reported that such a configuration would lead to an inaccurate prediction of the DOA. The development of new technologies that are convenient to use in the operating room can provide accurate and objective monitoring of anesthesia. Beginning with a brief introduction of the nascent technique of the brain connectome, this review summarizes recent network studies on anesthesia and consciousness.

Moreover, we have identified potential research directions to extend the current studies with regard to embracing new technologies (including machine learning and multimodal neuroimaging). We believe that incorporating network analysis with a portable EEG system will lead to a promising solution for accurate anesthesia monitoring in clinical applications.

## Acknowledgments

This work was supported by the Zhejiang Provincial Natural Science Foundation of China (LGF19H090023), the National Natural Science Foundation of China (81801785 and 82172056), the National Key Research and Development Program of China (2019YFC1711800), and the Key Research and Development Program of Shanxi (2020ZDLSF04-03). This work was partly supported by the grants from the Zhejiang Lab (2019KE0AD01 and 2021KE0AB04), the Zhejiang University Global Partnership Fund (100000-11320), the Shanghai Municipal Science and Technology Major Project (2021SHZDZX0100), and the Fundamental Research Funds for the Central Universities.

## Compliance with ethics guidelines

Jun Liu, Kangli Dong, Yi Sun, Ioannis Kakkos, Fan Huang, Guozheng Wang, Peng Qi, Xing Chen, Delin Zhang, Anastasios Bezerianos, and Yu Sun declare that they have no conflict of interest or financial conflicts to disclose.

## References

[1] Antognini JF, Carstens E. *In vivo* characterization of clinical anaesthesia and its components. Br J Anaesth 2002;89(1):156–66.
[2] Thompson AJ, Alqazzaz M, Ulens C, Lummis SC. The pharmacological profile of ELIC, a prokaryotic GABA-gated receptor. Neuropharmacology 2012;63(4):761–7.
[3] Petrenko AB, Yamakura T, Sakimura K, Baba H. Defining the role of NMDA receptors in anesthesia: are we there yet? Eur J Pharmacol 2014;723:29–37.
[4] Steinberg EA, Wafford KA, Brickley SG, Franks NP, Wisden W. The role of K2p channels in anaesthesia and sleep. Pflugers Arch 2015;467(5):907–16.
[5] Franks NP. General anaesthesia: from molecular targets to neuronal pathways of sleep and arousal. Nat Rev Neurosci 2008;9(5):370–86.
[6] Nd EE, Saidman LJ, Brandstater B. Minimum alveolar anesthetic concentration: a standard of anesthetic potency. Anesthesiology 1965;26(6):756–63.
[7] Roizen MF, Horrigan RW, Frazer BM. Anesthetic doses blocking adrenergic (stress) and cardiovascular responses to incision—MAC BAR. Anesthesiology 1981;54(5):390–8.
[8] Prys-Roberts C. Anaesthesia: a practical or impractical construct? Br J Anaesth 1987;59(11):1341–5.
[9] Katoh T, Ikeda K. The effects of fentanyl on sevoflurane requirements for loss of consciousness and skin incision. Anesthesiology 1998;88(1):18–24.
[10] Meuret P, Backman SB, Bonhomme V, Plourde G, Fiset P. Physostigmine reverses propofol-induced unconsciousness and attenuation of the auditory steady state response and bispectral index in human volunteers. Anesthesiology 2000;93(3):708–17.
[11] Mhuircheartaigh RN, Rosenorn-Lanng D, Wise R, Jbabdi S, Rogers R, Tracey I. Cortical and subcortical connectivity changes during decreasing levels of consciousness in humans: a functional magnetic resonance imaging study using propofol. J Neurosci 2010;30(27):9095–102.
[12] White NS, Alkire MT. Impaired thalamocortical connectivity in humans during general-anesthetic-induced unconsciousness. Neuroimage 2003;19(2 Pt 1):402–11.
[13] Alkire MT, Haier RJ, Fallon JH. Toward a unified theory of narcosis: brain imaging evidence for a thalamocortical switch as the neurophysiologic basis of anesthetic-induced unconsciousness. Conscious Cogn 2000;9(3):370–86.
[14] Franks NP, Zecharia AY. Sleep and general anesthesia. Can J Anaesth 2011;58(2):139–48.
[15] Luo T, Leung LS. Basal forebrain histaminergic transmission modulates electroencephalographic activity and emergence from isoflurane anesthesia. Anesthesiology 2009;111(4):725–33.
[16] Alkire MT. Probing the mind: anesthesia and neuroimaging. Clin Pharmacol Ther 2008;84(1):149–52.
[17] Ferrarelli F, Massimini M, Sarasso S, Casali A, Riedner BA, Angelini G, et al. Breakdown in cortical effective connectivity during midazolam-induced loss of consciousness. Proc Natl Acad Sci USA 2010;107(6):2681–6.
[18] Alkire MT, Hudetz AG, Tononi G. Consciousness and anesthesia. Science 2008;322(5903):876–80.
[19] Alkire MT, Miller J. General anesthesia and the neural correlates of consciousness. Prog Brain Res 2005;150:229–44.
[20] Ward LM. The thalamic dynamic core theory of conscious experience. Conscious Cogn 2011;20(2):464–86.
[21] Velly LJ, Rey MF, Bruder NJ, Gouvitsos FA, Witjas T, Regis JM, et al. Differential dynamic of action on cortical and subcortical structures of anesthetic agents during induction of anesthesia. Anesthesiology 2007;107(2):202–12.
[22] Huupponen E, Maksimow A, Lapinlampi P, Särkelä M, Saastamoinen A, Snapir A, et al. Electroencephalogram spindle activity during dexmedetomidine sedation and physiological sleep. Acta Anaesthesiol Scand 2008;52(2):289–94.
[23] Zecharia AY, Franks NP. General anesthesia and ascending arousal pathways. Anesthesiology 2009;111(4):695–6.
[24] Sanders RD, Tononi G, Laureys S, Sleigh JW, Warner DS. Unresponsiveness ≠ unconsciousness. Anesthesiology 2012;116(4):946–59.
[25] Ramsay MA, Savege TM, Simpson BR, Goodwin R. Controlled sedation with alphaxalone–alphadolone. BMJ 1974;2(5920):656–9.
[26] Devlin JW, Boleski G, Mlynarek M, Nerenz DR, Peterson E, Jankowski M, et al. Motor Activity Assessment Scale: a valid and reliable sedation scale for use with mechanically ventilated patients in an adult surgical intensive care unit. Crit Care Med 1999;27(7):1271–5.
[27] Riker RR, Picard JT, Fraser GL. Prospective evaluation of the Sedation–Agitation Scale for adult critically ill patients. Crit Care Med 1999;27(7):1325–9.
[28] Greicius MD, Krasnow B, Reiss AL, Menon V. Functional connectivity in the resting brain: a network analysis of the default mode hypothesis. Proc Natl Acad Sci USA 2003;100(1):253–8.
[29] Kerssens C, Hamann S, Peltier S, Hu XP, Byas-Smith MG, Sebel PS. Attenuated brain response to auditory word stimulation with sevoflurane: a functional magnetic resonance imaging study in humans. Anesthesiology 2005;103(1):11–9.
[30] Dueck MH, Petzke F, Gerbershagen HJ, Paul M, Hesselmann V, Girnus R, et al. Propofol attenuates responses of the auditory cortex to acoustic stimulation in a dose-dependent manner: a FMRI study. Acta Anaesthesiol Scand 2005;49(6):784–91.
[31] Plourde G, Belin P, Chartrand D, Fiset P, Backman SB, Xie G, et al. Cortical processing of complex auditory stimuli during alterations of consciousness with the general anesthetic propofol. Anesthesiology 2006;104(3):448–57.
[32] Ramani R, Qiu M, Constable RT. Sevoflurane 0.25 MAC preferentially affects higher order association areas: a functional magnetic resonance imaging study in volunteers. Anesth Analg 2007;105(3):648–55.
[33] Jonckers E, Delgado y Palacios R, Shah D, Guglielmetti C, Verhoye M, van der Linden A. Different anesthesia regimes modulate the functional connectivity outcome in mice. Magn Reson Med 2014;72(4):1103–12.
[34] Vincent JL, Patel GH, Fox MD, Snyder AZ, Baker JT, Van Essen DC, et al. Intrinsic functional architecture in the anaesthetized monkey brain. Nature 2007;447(7140):83–6.
[35] Fiset P, Paus T, Daloze T, Plourde G, Meuret P, Bonhomme V, et al. Brain mechanisms of propofol-induced loss of consciousness in humans: a positron emission tomographic study. J Neurosci 1999;19(13):5506–13.
[36] Liu X, Lauer KK, Ward BD, Li SJ, Hudetz AG. Differential effects of deep sedation with propofol on the specific and nonspecific thalamocortical systems: a functional magnetic resonance imaging study. Anesthesiology 2013;118(1):59–69.
[37] Liu X, Lauer KK, Ward BD, Rao SM, Li SJ, Hudetz AG. Propofol disrupts functional interactions between sensory and high-order processing of auditory verbal memory. Hum Brain Mapp 2012;33(10):2487–98.
[38] Peltier SJ, Kerssens C, Hamann SB, Sebel PS, Byas-Smith M, Hu X. Functional connectivity changes with concentration of sevoflurane anesthesia. NeuroReport 2005;16(3):285–8.
[39] Alkire MT, Haier RJ, Barker SJ, Shah NK, Wu JC, Kao YJ. Cerebral metabolism during propofol anesthesia in humans studied with positron emission tomography. Anesthesiology 1995;82(2):393–403.
[40] Alkire MT, Pomfrett CJ, Haier RJ, Gianzero MV, Chan CM, Jacobsen BP, et al. Functional brain imaging during anesthesia in humans: effects of halothane on global and regional cerebral glucose metabolism. Anesthesiology 1999;90(3):701–9.
[41] Alkire MT, Haier RJP, Shah NKM, Anderson CTM. Positron emission tomography study of regional cerebral metabolism in humans during isoflurane anesthesia. Anesthesiology 1997;86(3):549–57.
[42] Bonhomme V, Fiset P, Meuret P, Backman S, Plourde G, Paus T, et al. Propofol anesthesia and cerebral blood flow changes elicited by vibrotactile stimulation: a positron emission tomography study. J Neurophysiol 2001;85(3):1299–308.
[43] Owen-Reece H, Elwell CE, Harkness W, Goldstone J, Delpy DT, Wyatt JS, et al. Use of near infrared spectroscopy to estimate cerebral blood flow in conscious and anaesthetized adult subjects. Br J Anaesth 1996;76(1):43–8.
[44] Lovell AT, Owen-Reece H, Elwell CE, Smith M, Goldstone JC. Continuous measurement of cerebral oxygenation by near infrared spectroscopy during induction of anesthesia. Anesth Analg 1999;88(3):554–8.
[45] Curtin A, Izzetoglu K, Reynolds J, Menon R, Izzetoglu M, Osbakken M, et al. Functional near-infrared spectroscopy for the measurement of propofol effects in conscious sedation during outpatient elective colonoscopy. Neuroimage 2014;85(Pt 1):626–36.

[46] Kanemaru Y, Nishikawa K, Goto F. Bispectral index and regional cerebral oxygen saturation during propofol/$N_2O$ anesthesia. Can J Anaesth 2006;53(4):363–9.
[47] Kasuya Y, Govinda R, Rauch S, Mascha EJ, Sessler DI, Turan A. The correlation between bispectral index and observational sedation scale in volunteers sedated with dexmedetomidine and propofol. Anesth Analg 2009;109(6):1811–5.
[48] Hans P, Dewandre PY, Brichant JF, Bonhomme V. Comparative effects of ketamine on bispectral index and spectral entropy of the electroencephalogram under sevoflurane anaesthesia. Br J Anaesth 2005;94(3):336–40.
[49] Hirota K, Kubota T, Ishihara H, Matsuki A. The effects of nitrous oxide and ketamine on the bispectral index and 95% spectral edge frequency during propofol–fentanyl anaesthesia. Eur J Anaesthesiol 1999;16(11):779–83.
[50] Chalela R, Gallart L, Pascual-Guardia S, Sancho-Muñoz A, Gea J, Orozco-Levi M. Bispectral index in hypercapnic encephalopathy associated with COPD exacerbation: a pilot study. Int J Chron Obstruct Pulmon Dis 2018;13:2961–7.
[51] Avidan MS, Zhang L, Burnside BA, Finkel KJ, Searleman AC, Selvidge JA, et al. Anesthesia awareness and the bispectral index. N Engl J Med 2008;358(11):1097–108.
[52] Davidson AJ, McCann ME, Devavaram P, Auble SA, Sullivan LJ, Gillis JM, et al. The differences in the bispectral index between infants and children during emergence from anesthesia after circumcision surgery. Anesth Analg 2001;93(2):326–30.
[53] Degoute CS, Macabeo C, Dubreuil C, Duclaux R, Banssillon V. EEG bispectral index and hypnotic component of anaesthesia induced by sevoflurane: comparison between children and adults. Br J Anaesth 2001;86(2):209–12.
[54] Denman WT, Swanson EL, Rosow D, Ezbicki K, Connors PD, Rosow CE. Pediatric evaluation of the bispectral index (BIS) monitor and correlation of BIS with end-tidal sevoflurane concentration in infants and children. Anesth Analg 2000;90(4):872–7.
[55] Kim HS, Oh AY, Kim CS, Kim SD, Seo KS, Kim JH. Correlation of bispectral index with end-tidal sevoflurane concentration and age in infants and children. Br J Anaesth 2005;95(3):362–6.
[56] Ibrahim AE, Taraday JK, Kharasch ED. Bispectral index monitoring during sedation with sevoflurane, midazolam, and propofol. Anesthesiology 2001;95(5):1151–9.
[57] Hart SM, Buchannan CR, Sleigh JW. A failure of M-Entropy™ to correctly detect burst suppression leading to sevoflurane overdosage. Anaesth Intensive Care 2009;37(6):1002–4.
[58] Viertiö-Oja H, Maja V, Särkelä M, Talja P, Tenkanen N, Tolvanen-Laakso H, et al. Description of the Entropy™ algorithm as applied in the Datex-Ohmeda 5/5™ Entropy Module. Acta Anaesthesiol Scand 2004;48(2):154–61.
[59] Purdon PL, Sampson A, Pavone KJ, Brown EN. Clinical electroencephalography for anesthesiologists: part I: background and basic signatures. Anesthesiology 2015;123(4):937–60.
[60] Akeju O, Pavone KJ, Westover MB, Vazquez R, Prerau MJ, Harrell PG, et al. A comparison of propofol- and dexmedetomidine-induced electroencephalogram dynamics using spectral and coherence analysis. Anesthesiology 2014;121(5):978–89.
[61] Akeju O, Song AH, Hamilos AE, Pavone KJ, Flores FJ, Brown EN, et al. Electroencephalogram signatures of ketamine anesthesia-induced unconsciousness. Clin Neurophysiol 2016;127(6):2414–22.
[62] Purdon PL, Pavone KJ, Akeju O, Smith AC, Sampson AL, Lee J, et al. The Ageing Brain: age-dependent changes in the electroencephalogram during propofol and sevoflurane general anaesthesia. Br J Anaesth 2015;115(Suppl 1):i46–57.
[63] Nash CL Jr, Lorig RA, Schatzinger LA, Brown RH. Spinal cord monitoring during operative treatment of the spine. Clin Orthop Relat Res 1977;126:100–5.
[64] Tooley MA, Greenslade GL, Prys-Roberts C. Concentration-related effects of propofol on the auditory evoked response. Br J Anaesth 1996;77(6):720–6.
[65] Doi M, Gajraj RJ, Mantzaridis H, Kenny GN. Relationship between calculated blood concentration of propofol and electrophysiological variables during emergence from anaesthesia: comparison of bispectral index, spectral edge frequency, median frequency and auditory evoked potential index. Br J Anaesth 1997;78(2):180–4.
[66] Gajraj RJ, Doi M, Mantzaridis H, Kenny GN. Comparison of bispectral EEG analysis and auditory evoked potentials for monitoring depth of anaesthesia during propofol anaesthesia. Br J Anaesth 1999;82(5):672–8.
[67] Barr G, Anderson RE, Jakobsson JG. A study of bispectral analysis and auditory evoked potential indices during propofol-induced hypnosis in volunteers: the effect of an episode of wakefulness on explicit and implicit memory. Anaesthesia 2001;56(9):888–93.
[68] Thornton C, Konieczko KM, Knight AB, Kaul B, Jones JG, Dore CJ, et al. Effect of propofol on the auditory evoked response and oesophageal contractility. Br J Anaesth 1989;63(4):411–7.
[69] Karasawa H, Sakaida K, Noguchi S, Hatayama K, Naito H, Hirota N, et al. Intracranial electroencephalographic changes in deep anesthesia. Clin Neurophysiol 2001;112(1):25–30.
[70] Boly M, Moran R, Murphy M, Boveroux P, Bruno MA, Noirhomme Q, et al. Connectivity changes underlying spectral EEG changes during propofol-induced loss of consciousness. J Neurosci 2012;32(20):7082–90.
[71] Lee U, Kim S, Noh GJ, Choi BM, Hwang E, Mashour GA. The directionality and functional organization of frontoparietal connectivity during consciousness and anesthesia in humans. Conscious Cogn 2009;18(4):1069–78.
[72] Lee U, Ku S, Noh G, Baek S, Choi B, Mashour GA. Disruption of frontal–parietal communication by ketamine, propofol, and sevoflurane. Anesthesiology 2013;118(6):1264–75.
[73] Purdon PL, Pierce ET, Mukamel EA, Prerau MJ, Walsh JL, Wong KFK, et al. Electroencephalogram signatures of loss and recovery of consciousness from propofol. Proc Natl Acad Sci USA 2013;110(12):E1142–51.
[74] Huang Y, Wu D, Bahuri NFA, Wang S, Hyam JA, Yarrow S, et al. Spectral and phase-amplitude coupling signatures in human deep brain oscillations during propofol-induced anaesthesia. Br J Anaesth 2018;121(1):303–13.
[75] Hudetz AG. General anesthesia and human brain connectivity. Brain Connect 2012;2(6):291–302.
[76] Bassett DS, Sporns O. Network neuroscience. Nat Neurosci 2017;20(3):353–64.
[77] Michel CM, Murray MM, Lantz G, Gonzalez S, Spinelli L, Grave de Peralta R. EEG source imaging. Clin Neurophysiol 2004;115(10):2195–222.
[78] Friston KJ. Functional and effective connectivity: a review. Brain Connect 2011;1(1):13–36.
[79] Friston KJ. Functional and effective connectivity in neuroimaging: a synthesis. Hum Brain Mapp 1994;2(1–2):56–78.
[80] Paul LN, Ramesh S, et al. EEG coherency. I: statistics, reference electrode, volume conduction, laplacians, cortical imaging, and interpretation at multiple scales. Electroencephalogr Clin Neurophysiol 1997;103(5):499–515.
[81] Stam CJ, Nolte G, Daffertshofer A. Phase lag index: assessment of functional connectivity from multi channel EEG and MEG with diminished bias from common sources. Hum Brain Mapp 2007;28(11):1178–93.
[82] Vinck M, Oostenveld R, van Wingerden M, Battaglia F, Pennartz CM. An improved index of phase-synchronization for electrophysiological data in the presence of volume-conduction, noise and sample-size bias. Neuroimage 2011;55(4):1548–65.
[83] Bruña R, Maestú F, Pereda E. Phase locking value revisited: teaching new tricks to an old dog. J Neural Eng 2018;15(5):056011.
[84] Lachaux JP, Rodriguez E, Martinerie J, Varela FJ. Measuring phase synchrony in brain signals. Hum Brain Mapp 1999;8(4):194–208.
[85] Lee H, Noh GJ, Joo P, Choi BM, Silverstein BH, Kim M, et al. Diversity of functional connectivity patterns is reduced in propofol-induced unconsciousness. Hum Brain Mapp 2017;38(10):4980–95.
[86] Vinck M, van Wingerden M, Womelsdorf T, Fries P, Pennartz CM. The pairwise phase consistency: a bias-free measure of rhythmic neuronal synchronization. Neuroimage 2010;51(1):112–22.
[87] Nolte G, Ziehe A, Nikulin VV, Schlögl A, Krämer N, Brismar T, et al. Robustly estimating the flow direction of information in complex physical systems. Phys Rev Lett 2008;100(23):234101.
[88] Hipp JF, Hawellek DJ, Corbetta M, Siegel M, Engel AK. Large-scale cortical correlation structure of spontaneous oscillatory activity. Nat Neurosci 2012;15(6):884–90.
[89] Kraskov A, Stögbauer H, Grassberger P. Estimating mutual information. Phys Rev E Stat Nonlin Soft Matter Phys 2004;69(6 Pt 2):066138.
[90] Frenzel S, Pompe B. Partial mutual information for coupling analysis of multivariate time series. Phys Rev Lett 2007;99(20):204101.
[91] Lobier M, Siebenhühner F, Palva S, Palva JM. Phase transfer entropy: a novel phase-based measure for directed connectivity in networks coupled by oscillatory interactions. Neuroimage 2014;85(Pt 2):853–72.
[92] Baccala LA, Sameshima K, Takahashi DY. Generalized partial directed coherence. In: Proceedings of 2007 15th International Conference on Digital Signal Processing; 2007 Jul 1–4; Cardiff, UK. IEEE; 2007. p. 163–6.
[93] Schelter B, Timmer J, Eichler M. Assessing the strength of directed influences among neural signals using renormalized partial directed coherence. J Neurosci Methods 2009;179(1):121–30.
[94] Baccalá LA, Sameshima K. Partial directed coherence: a new concept in neural structure determination. Biol Cybern 2001;84(6):463–74.
[95] Korzeniewska A, Mańczak M, Kamiński M, Blinowska KJ, Kasicki S. Determination of information flow direction among brain structures by a modified directed transfer function (dDTF) method. J Neurosci Methods 2003;125(1–2):195–207.
[96] Kamiński MJ, Blinowska KJ. A new method of the description of the information flow in the brain structures. Biol Cybern 1991;65(3):203–10.
[97] Özkurt TE, Schnitzler A. A critical note on the definition of phase-amplitude cross-frequency coupling. J Neurosci Methods 2011;201(2):438–43.
[98] Granger CW. Investigating causal relations by econometric models and cross-spectral methods. Econometrica 1969;37(3):424–38.
[99] Bastos AM, Schoffelen JM. A tutorial review of functional connectivity analysis methods and their interpretational pitfalls. Front Syst Neurosci 2016;9:175.
[100] He B, Astolfi L, Valdés-Sosa PA, Marinazzo D, Palva S, Bénar CG, et al. Electrophysiological brain connectivity: theory and implementation. IEEE Trans Biomed Eng 2019;66(7):2115–37.
[101] Sakkalis V. Review of advanced techniques for the estimation of brain connectivity measured with EEG/MEG. Comput Biol Med 2011;41(12):1110–7.
[102] Watts DJ, Strogatz SH. Collective dynamics of 'small-world' networks. Nature 1998;393(6684):440–2.
[103] Boccaletti S, Latora V, Moreno Y, Chavez M, Hwang DU. Complex networks: structure and dynamics. Phys Rep 2006;424(4–5):175–308.
[104] Farahani FV, Karwowski W, Lighthall NR. Application of graph theory for identifying connectivity patterns in human brain networks: a systematic review. Front Neurosci 2019;13:585.

[105] Bullmore E, Sporns O. Complex brain networks: graph theoretical analysis of structural and functional systems. Nat Rev Neurosci 2009;10(3):186–98.
[106] Rubinov M, Sporns O. Complex network measures of brain connectivity: uses and interpretations. Neuroimage 2010;52(3):1059–69.
[107] Wang J, Wang X, Xia M, Liao X, Evans A, He Y. GRETNA: a graph theoretical network analysis toolbox for imaging connectomics. Front Hum Neurosci 2015;9:386.
[108] Hosseini SM, Hoeft F, Kesler SR. GAT: a graph-theoretical analysis toolbox for analyzing between-group differences in large-scale structural and functional brain networks. PLoS ONE 2012;7(7):e40709.
[109] Kruschwitz JD, List D, Waller L, Rubinov M, Walter H. GraphVar: a user-friendly toolbox for comprehensive graph analyses of functional brain connectivity. J Neurosci Methods 2015;245:107–15.
[110] Mijalkov M, Kakaei E, Pereira JB, Westman E, Volpe G; the Alzheimer's Disease Neuroimaging Initiative. BRAPH: a graph theory software for the analysis of brain connectivity. PLoS One 2017;12(8):e0178798.
[111] Niso G, Bruña R, Pereda E, Gutiérrez R, Bajo R, Maestú F, et al. HERMES: towards an integrated toolbox to characterize functional and effective brain connectivity. Neuroinformatics 2013;11(4):405–34.
[112] Schwanghart W, Kuhn N. TopoToolbox: a set of Matlab functions for topographic analysis. Environ Model Softw 2010;25(6):770–81.
[113] Whitfield-Gabrieli S, Nieto-Castanon A. Conn: a functional connectivity toolbox for correlated and anticorrelated brain networks. Brain Connect 2012;2(3):125–41.
[114] Rabinovich MI, Friston KJ, Varona P. Principles of brain dynamics: global state interactions. Cambridge: MIT Press; 2012.
[115] Chang C, Glover GH. Time-frequency dynamics of resting-state brain connectivity measured with fMRI. Neuroimage 2010;50(1):81–98.
[116] Calhoun VD, Miller R, Pearlson G, Adalı T. The chronnectome: time-varying connectivity networks as the next frontier in fMRI data discovery. Neuron 2014;84(2):262–74.
[117] Hutchison RM, Womelsdorf T, Allen EA, Bandettini PA, Calhoun VD, Corbetta M, et al. Dynamic functional connectivity: promise, issues, and interpretations. Neuroimage 2013;80:360–78.
[118] Lurie DJ, Kessler D, Bassett DS, Betzel RF, Breakspear M, Kheilholz S, et al. Questions and controversies in the study of time-varying functional connectivity in resting fMRI. Netw Neurosci 2020;4(1):30–69.
[119] Preti MG, Bolton TA, Van De Ville D. The dynamic functional connectome: state-of-the-art and perspectives. Neuroimage 2017;160:41–54.
[120] Smith SM, Miller KL, Salimi-Khorshidi G, Webster M, Beckmann CF, Nichols TE, et al. Network modelling methods for FMRI. Neuroimage 2011;54(2):875–91.
[121] Fu Z, Du Y, Calhoun VD. The dynamic functional network connectivity analysis framework. Engineering 2019;5(2):190–3.
[122] Hudetz AG, Mashour GA. Disconnecting consciousness: is there a common anesthetic end-point? Anesth Analg 2016;123(5):1228–40.
[123] Chennu S, O'Connor S, Adapa R, Menon DK, Bekinschtein TA. Brain connectivity dissociates responsiveness from drug exposure during propofol-induced transitions of consciousness. PLOS Comput Biol 2016;12(1):e1004669.
[124] Kim M, Mashour GA, Moraes SB, Vanini G, Tarnal V, Janke E, et al. Functional and topological conditions for explosive synchronization develop in human brain networks with the onset of anesthetic-induced unconsciousness. Front Comput Neurosci 2016;10:1.
[125] Lee M, Sanders RD, Yeom SK, Won DO, Seo KS, Kim HJ, et al. Network properties in transitions of consciousness during propofol-induced sedation. Sci Rep 2017;7(1):16791.
[126] Numan T, Slooter AJC, van der Kooi AW, Hoekman AML, Suyker WJL, Stam CJ, et al. Functional connectivity and network analysis during hypoactive delirium and recovery from anesthesia. Clin Neurophysiol 2017;128(6):914–24.
[127] Ryu JH, Kim PJ, Kim HG, Koo YS, Shin TJ. Investigating the effects of nitrous oxide sedation on frontal–parietal interactions. Neurosci Lett 2017;651:9–15.
[128] Cha KM, Choi BM, Noh GJ, Shin HC. Novel methods for measuring depth of anesthesia by quantifying dominant information flow in multichannel EEGs. Comput Intell Neurosci 2017;2017:3521261.
[129] Blain-Moraes S, Tarnal V, Vanini G, Bel-Behar T, Janke E, Picton P, et al. Network efficiency and posterior alpha patterns are markers of recovery from general anesthesia: a high-density electroencephalography study in healthy volunteers. Front Hum Neurosci 2017;11:328.
[130] Vlisides PE, Bel-Bahar T, Lee U, Li D, Kim H, Janke E, et al. Neurophysiologic correlates of ketamine sedation and anesthesia: a high-density electroencephalography study in healthy volunteers. Anesthesiology 2017;127(1):58–69.
[131] Kim H, Hudetz AG, Lee J, Mashour GA, Lee U, Avidan MS, et al. Estimating the integrated information measure phi from high-density electroencephalography during states of consciousness in humans. Front Hum Neurosci 2018;12:42.
[132] Lee H, Golkowski D, Jordan D, Berger S, Ilg R, Lee J, et al.; the ReCCognition Study Group. Relationship of critical dynamics, functional connectivity, and states of consciousness in large-scale human brain networks. Neuroimage 2019;188:228–38.
[133] Sanders RD, Banks MI, Darracq M, Moran R, Sleigh J, Gosseries O, et al. Propofol-induced unresponsiveness is associated with impaired feedforward connectivity in cortical hierarchy. Br J Anaesth 2018;121(5):1084–96.
[134] Zhang Y, Wang C, Wang Y, Yan F, Wang Q, Huang L. Investigating dynamic functional network patterns after propofol-induced loss of consciousness. Clin Neurophysiol 2019;130(3):331–40.
[135] Li D, Vlisides PE, Kelz MB, Avidan MS, Mashour GA; the ReCCognition Study Group. Dynamic cortical connectivity during general anesthesia in healthy volunteers. Anesthesiology 2019;130(6):870–84.
[136] Lioi G, Bell SL, Smith DC, Simpson DM. Measuring depth of anaesthesia using changes in directional connectivity: a comparison with auditory middle latency response and estimated bispectral index during propofol anaesthesia. Anaesthesia 2019;74(3):321–32.
[137] Pappas I, Cornelissen L, Menon DK, Berde CB, Stamatakis EA. δ-oscillation correlates of anesthesia-induced unconsciousness in large-scale brain networks of human infants. Anesthesiology 2019;131(6):1239–53.
[138] Afshani F, Shalbaf A, Shalbaf R, Sleigh J. Frontal-temporal functional connectivity of EEG signal by standardized permutation mutual information during anesthesia. Cogn Neurodyn 2019;13(6):531–40.
[139] Numan T, van Dellen E, Vleggaar FP, van Vlieberghe P, Stam CJ, Slooter AJC. Resting state EEG characteristics during sedation with midazolam or propofol in older subjects. Clin EEG Neurosci 2019;50(6):436–43.
[140] Ki S, Kim KM, Lee YH, Bang JY, Choi BM, Noh GJ. Phase lag entropy as a hypnotic depth indicator during propofol sedation. Anaesthesia 2019;74(8):1033–40.
[141] Banks MI, Krause BM, Endemann CM, Campbell DI, Kovach CK, Dyken ME, et al. Cortical functional connectivity indexes arousal state during sleep and anesthesia. Neuroimage 2020;211:116627.
[142] Liang Z, Cheng L, Shao S, Jin X, Yu T, Sleigh JW, et al. Information integration and mesoscopic cortical connectivity during propofol anesthesia. Anesthesiology 2020;132(3):504–24.
[143] Li D, Puglia MP, Lapointe AP, Ip KI, Zierau M, McKinney A, et al. Age-related changes in cortical connectivity during surgical anesthesia. Front Aging Neurosci 2020;11:371.
[144] Pullon RM, Yan L, Sleigh JW, Warnaby CE. Granger causality of the electroencephalogram reveals abrupt global loss of cortical information flow during propofol-induced loss of responsiveness. Anesthesiology 2020;133(4):774–86.
[145] Halder S, Juel BE, Nilsen AS, Raghavan LV, Storm JF. Changes in measures of consciousness during anaesthesia of one hemisphere (Wada test). Neuroimage 2021;226:117566.
[146] Sattin D, Duran D, Visintini S, Schiaffi E, Panzica F, Carozzi C, et al. Analyzing the loss and the recovery of consciousness: functional connectivity patterns and changes in heart rate variability during propofol-induced anesthesia. Front Syst Neurosci 2021;15:652080.
[147] Zhao X, Wang Y, Zhang Y, Wang H, Ren J, Yan F, et al. Propofol-induced anesthesia alters corticocortical functional connectivity in the human brain: an EEG source space analysis. Neurosci Bull 2021;37(6):563–8.
[148] Duclos C, Maschke C, Mahdid Y, Berkun K, Castanheira JDS, Tarnal V, et al. Differential classification of states of consciousness using envelope- and phase-based functional connectivity. Neuroimage 2021;237:118171.
[149] Chamadia S, Pedemonte JC, Hahm EY, Mekonnen J, Ibala R, Gitlin J, et al. Delta oscillations phase limit neural activity during sevoflurane anesthesia. Commun Biol 2019;2(1):415.
[150] Liang Z, Ren N, Wen X, Li H, Guo H, Ma Y, et al. Age-dependent cross frequency coupling features from children to adults during general anesthesia. Neuroimage 2021;240:118372.
[151] Mukamel EA, Pirondini E, Babadi B, Wong KFK, Pierce ET, Harrell PG, et al. A transition in brain state during propofol-induced unconsciousness. J Neurosci 2014;34(3):839–45.
[152] Jensen O, Colgin LL. Cross-frequency coupling between neuronal oscillations. Trends Cogn Sci 2007;11(7):267–9.
[153] Canolty RT, Knight RT. The functional role of cross-frequency coupling. Trends Cogn Sci 2010;14(11):506–15.
[154] Schreiber T. Measuring information transfer. Phys Rev Lett 2000;85(2):461–4.
[155] Vlisides PE, Li D, Zierau M, Lapointe AP, Ip KI, McKinney AM, et al. Dynamic cortical connectivity during general anesthesia in surgical patients. Anesthesiology 2019;130(6):885–97.
[156] Ma Y, Hamilton C, Zhang N. Dynamic connectivity patterns in conscious and unconscious brain. Brain Connect 2017;7(1):1–12.
[157] Schroeder KE, Irwin ZT, Gaidica M, Nicole Bentley J, Patil PG, Mashour GA, et al. Disruption of corticocortical information transfer during ketamine anesthesia in the primate brain. Neuroimage 2016;134:459–65.
[158] Guldenmund P, Gantner IS, Baquero K, Das T, Demertzi A, Boveroux P, et al. Propofol-induced frontal cortex disconnection: a study of resting-state networks, total brain connectivity, and mean BOLD signal oscillation frequencies. Brain Connect 2016;6(3):225–37.
[159] Ranft A, Golkowski D, Kiel T, Riedl V, Kohl P, Rohrer G, et al. Neural correlates of sevoflurane-induced unconsciousness identified by simultaneous functional magnetic resonance imaging and electroencephalography. Anesthesiology 2016;125(5):861–72.
[160] Wu T, Grandjean J, Bosshard SC, Rudin M, Reutens D, Jiang T. Altered regional connectivity reflecting effects of different anaesthesia protocols in the mouse brain. Neuroimage 2017;149:190–9.
[161] Luppi AI, Craig MM, Pappas I, Finoia P, Williams GB, Allanson J, et al. Consciousness-specific dynamic interactions of brain integration and functional diversity. Nat Commun 2019;10(1):4616.

[162] Paasonen J, Stenroos P, Salo RA, Kiviniemi V, Gröhn O. Functional connectivity under six anesthesia protocols and the awake condition in rat brain. Neuroimage 2018;172:9–20.
[163] Huang Z, Tarnal V, Vlisides PE, Janke EL, McKinney AM, Picton P, et al. Asymmetric neural dynamics characterize loss and recovery of consciousness. Neuroimage 2021;236:118042.
[164] Standage D, Areshenkoff CN, Nashed JY, Hutchison RM, Hutchison M, Heinke D, et al. Dynamic reconfiguration, fragmentation, and integration of whole-brain modular structure across depths of unconsciousness. Cereb Cortex 2020;30(10):5229–41.
[165] Luppi AI, Golkowski D, Ranft A, Ilg R, Jordan D, Menon DK, et al. Brain network integration dynamics are associated with loss and recovery of consciousness induced by sevoflurane. Hum Brain Mapp 2021;42(9):2802–22.
[166] Areshenkoff CN, Nashed JY, Hutchison RM, Hutchison M, Levy R, Cook DJ, et al. Muting, not fragmentation, of functional brain networks under general anesthesia. Neuroimage 2021;231:117830.
[167] Vatansever D, Schröter M, Adapa RM, Bullmore ET, Menon DK, Stamatakis EA. Reorganisation of brain hubs across altered states of consciousness. Sci Rep 2020;10(1):3402.
[168] Wang S, Li Y, Qiu S, Zhang C, Wang G, Xian J, et al. Reorganization of rich-clubs in functional brain networks during propofol-induced unconsciousness and natural sleep. Neuroimage Clin 2020;25:102188.
[169] Tsurugizawa T, Yoshimaru D. Impact of anaesthesia on static and dynamic functional connectivity in mice. NeuroImage 2021;241:118413.
[170] Yin D, Zhang Z, Wang Z, Zeljic K, Lv Q, Cai D, et al. Brain map of intrinsic functional flexibility in anesthetized monkeys and awake humans. Front Neurosci 2019;13:174.
[171] Golkowski D, Larroque SK, Vanhaudenhuyse A, Plenevaux A, Boly M, Di Perri C, et al. Changes in whole brain dynamics and connectivity patterns during sevoflurane- and propofol-induced unconsciousness identified by functional magnetic resonance imaging. Anesthesiology 2019;130(6):898–911.
[172] Barttfeld P, Uhrig L, Sitt JD, Sigman M, Jarraya B, Dehaene S. Signature of consciousness in the dynamics of resting-state brain activity. Proc Natl Acad Sci USA 2015;112(3):887–92.
[173] Schrouff J, Perlbarg V, Boly M, Marrelec G, Boveroux P, Vanhaudenhuyse A, et al. Brain functional integration decreases during propofol-induced loss of consciousness. Neuroimage 2011;57(1):198–205.
[174] Seeck M, Koessler L, Bast T, Leijten F, Michel C, Baumgartner C, et al. The standardized EEG electrode array of the IFCN. Clin Neurophysiol 2017;128(10):2070–7.
[175] Sohrabpour A, Lu Y, Kankirawatana P, Blount J, Kim H, He B. Effect of EEG electrode number on epileptic source localization in pediatric patients. Clin Neurophysiol 2015;126(3):472–80.
[176] Stoyell SM, Wilmskoetter J, Dobrota MA, Chinappen DM, Bonilha L, Mintz M, et al. High-density EEG in current clinical practice and opportunities for the future. J Clin Neurophysiol 2021;38(2):112–3.
[177] Christoff K, Irving ZC, Fox KC, Spreng RN, Andrews-Hanna JR. Mind-wandering as spontaneous thought: a dynamic framework. Nat Rev Neurosci 2016;17(11):718–31.
[178] Jenke R, Peer A, Buss M. Feature extraction and selection for emotion recognition from EEG. IEEE Trans Affect Comput 2014;5(3):327–39.
[179] Jin J, Miao Y, Daly I, Zuo C, Hu D, Cichocki A. Correlation-based channel selection and regularized feature optimization for MI-based BCI. Neural Netw 2019;118:262–70.
[180] Moffat AC, Murray AW, Fitch W. Opioid supplementation during propofol anaesthesia. The effects of fentanyl or alfentanil on propofol anaesthesia in daycase surgery. Anaesthesia 1989;44(8):644–7.
[181] Kim H, Lee U. Criticality as a determinant of integrated information Φ in human brain networks. Entropy 2019;21(10):981.
[182] Sebel PS, Bowdle TA, Ghoneim MM, Rampil IJ, Padilla RE, Gan TJ, et al. The incidence of awareness during anesthesia: a multicenter United States study. Anesth Analg 2004;99(3):833–9.
[183] Rundshagen I, Schröder T, Prichep LS, John ER, Kox WJ. Changes in cortical electrical activity during induction of anaesthesia with thiopental/fentanyl and tracheal intubation: a quantitative electroencephalographic analysis. Br J Anaesth 2004;92(1):33–8.
[184] Lallemand MA, Lentschener C, Mazoit JX, Bonnichon P, Manceau I, Ozier Y. Bispectral index changes following etomidate induction of general anaesthesia and orotracheal intubation. Br J Anaesth 2003;91(3):341–6.
[185] Kox WJ, von Heymann C, Heinze J, Prichep LS, John ER, Rundshagen I. Electroencephalographic mapping during routine clinical practice: cortical arousal during tracheal intubation? Anesth Analg 2006;102(3):825–31.
[186] Jensen EW, Valencia JF, López A, Anglada T, Agustí M, Ramos Y, et al. Monitoring hypnotic effect and nociception with two EEG-derived indices, qCON and qNOX, during general anaesthesia. Acta Anaesthesiol Scand 2014;58(8):933–41.
[187] Hartley C, Duff EP, Green G, Mellado GS, Worley A, Rogers R, et al. Nociceptive brain activity as a measure of analgesic efficacy in infants. Sci Transl Med 2017;9(388):eaah6122.
[188] Hernandez-Meza G, Izzetoglu M, Osbakken M, Green M, Abubakar H, Izzetoglu K. Investigation of optical neuro-monitoring technique for detection of maintenance and emergence states during general anesthesia. J Clin Monit Comput 2018;32(1):147–63.
[189] Hernandez-Meza G, Izzetoglu M, Sacan A, Green M, Izzetoglu K. Investigation of data-driven optical neuromonitoring approach during general anesthesia with sevoflurane. Neurophotonics 2017;4(4):041408.
[190] Liang Z, Gu Y, Duan X, Cheng L, Liang S, Tong Y, et al. Design of multichannel functional near-infrared spectroscopy system with application to propofol and sevoflurane anesthesia monitoring. Neurophotonics 2016;3(4):045001.
[191] Yeom SK, Won DO, Chi SI, Seo KS, Kim HJ, Müller KR, et al. Spatio–temporal dynamics of multimodal EEG-fNIRS signals in the loss and recovery of consciousness under sedation using midazolam and propofol. PLoS ONE 2017;12(11):e0187743.
[192] Mumtaz W, Rasheed S, Irfan A. Review of challenges associated with the EEG artifact removal methods. Biomed Signal Process Control 2021;68:102741.
[193] Islam MK, Rastegarnia A, Yang Z. Methods for artifact detection and removal from scalp EEG: a review. Neurophysiol Clin 2016;46(4–5):287–305.
[194] Dahaba AA. Different conditions that could result in the bispectral index indicating an incorrect hypnotic state. Anesth Analg 2005;101(3):765–73.
[195] García-Cossio E, Severens M, Nienhuis B, Duysens J, Desain P, Keijsers N, et al. Decoding sensorimotor rhythms during robotic-assisted treadmill walking for brain computer interface (BCI) applications. PLoS ONE 2015;10(12):e0137910.
[196] Samiee S, Baillet S. Time-resolved phase-amplitude coupling in neural oscillations. Neuroimage 2017;159:270–9.
[197] Lindquist MA, Xu Y, Nebel MB, Caffo BS. Evaluating dynamic bivariate correlations in resting-state fMRI: a comparison study and a new approach. Neuroimage 2014;101:531–46.
[198] Marusak HA, Calhoun VD, Brown S, Crespo LM, Sala-Hamrick K, Gotlib IH, et al. Dynamic functional connectivity of neurocognitive networks in children. Hum Brain Mapp 2017;38(1):97–108.
[199] Shakil S, Lee CH, Keilholz SD. Evaluation of sliding window correlation performance for characterizing dynamic functional connectivity and brain states. Neuroimage 2016;133:111–28.
[200] Betzel RF, Fukushima M, He Y, Zuo XN, Sporns O. Dynamic fluctuations coincide with periods of high and low modularity in resting-state functional brain networks. Neuroimage 2016;127:287–97.
[201] Du Y, Pearlson GD, Yu Q, He H, Lin D, Sui J, et al. Interaction among subsystems within default mode network diminished in schizophrenia patients: a dynamic connectivity approach. Schizophr Res 2016;170(1):55–65.
[202] Price T, Wee CY, Gao W, Shen D. Multiple-network classification of childhood autism using functional connectivity dynamics. Med Image Comput Assist Interv 2014;17(Pt 3):177–84.
[203] Wee CY, Yang S, Yap PT, Shen D; the Alzheimer's Disease Neuroimaging Initiative. Sparse temporally dynamic resting-state functional connectivity networks for early MCI identification. Brain Imaging Behav 2016;10(2):342–56.
[204] Yang S, Bornot JMS, Wong-Lin K, Prasad G. M/EEG-based bio-markers to predict the MCI and Alzheimer's disease: a review from the ML perspective. IEEE Trans Biomed Eng 2019;66(10):2924–35.
[205] Craik A, He Y, Contreras-Vidal JL. Deep learning for electroencephalogram (EEG) classification tasks: a review. J Neural Eng 2019;16(3):031001.
[206] Patel UK, Anwar A, Saleem S, Malik P, Rasul B, Patel K, et al. Artificial intelligence as an emerging technology in the current care of neurological disorders. J Neurol 2021;268(5):1623–42.
[207] Yu H, Lei X, Song Z, Liu C, Wang J. Supervised network-based fuzzy learning of EEG signals for Alzheimer's disease identification. IEEE Trans Fuzzy Syst 2019;28(1):60–71.
[208] Ho KC, Speier W, Zhang H, Scalzo F, El-Saden S, Arnold CW. A machine learning approach for classifying ischemic stroke onset time from imaging. IEEE Trans Med Imaging 2019;38(7):1666–76.
[209] Yu H, Zhu L, Cai L, Wang J, Liu J, Wang R, et al. Identification of Alzheimer's EEG with a WVG network-based fuzzy learning approach. Front Neurosci 2020;14:641.
[210] Li K, Wang J, Li S, Yu H, Zhu L, Liu J, et al. Feature extraction and identification of Alzheimer's disease based on latent factor of multi-channel EEG. IEEE Trans Neural Syst Rehabil Eng 2021;29:1557–67.
[211] Veselis RA, Reinsel R, Sommer S, Carlon G. Use of neural network analysis to classify electroencephalographic patterns against depth of midazolam sedation in intensive care unit patients. J Clin Monit 1991;7(3):259–67.
[212] Veselis RA, Reinsel R, Wronski M. Analytical methods to differentiate similar electroencephalographic spectra: neural network and discriminant analysis. J Clin Monit 1993;9(4):257–67.
[213] Ortolani O, Conti A, Di Filippo A, Adembri C, Moraldi E, Evangelisti A, et al. EEG signal processing in anaesthesia. Use of a neural network technique for monitoring depth of anaesthesia. Br J Anaesth 2002;88(5):644–8.
[214] Mirsadeghi M, Behnam H, Shalbaf R, Jelveh Moghadam H. Characterizing awake and anesthetized states using a dimensionality reduction method. J Med Syst 2016;40(1):13.
[215] Shalbaf A, Saffar M, Sleigh JW, Shalbaf R. Monitoring the depth of anesthesia using a new adaptive neurofuzzy system. IEEE J Biomed Health Inform 2018;22(3):671–7.
[216] Hashimoto DA, Witkowski E, Gao L, Meireles O, Rosman G. Artificial intelligence in anesthesiology: current techniques, clinical applications, and limitations. Anesthesiology 2020;132(2):379–94.
[217] Gao Z, Dang W, Wang X, Hong X, Hou L, Ma K, et al. Complex networks and deep learning for EEG signal analysis. Cogn Neurodyn 2021;15(3):369–88.
[218] Schneider G, Wagner K, Reeker W, Hänel F, Werner C, Kochs E. Bispectral index (BIS) may not predict awareness reaction to intubation in surgical patients. J Neurosurg Anesthesiol 2002;14(1):7–11.